# Effect of Mutation of Carboxyl Side-Chain Amino Acids Near the Heme on the Midpoint Potentials and Ligand Binding Constants of Nitrophorin 2 and Its NO, Histamine, and Imidazole Co…

**9 AUTHORS**, INCLUDING:

Robert E Berry
University of Massachusetts Dartmouth

**54** PUBLICATIONS   **559** CITATIONS

Maxim N Shokhirev
Salk Institute

**22** PUBLICATIONS   **166** CITATIONS

F(rances) Ann Walker
The University of Arizona

**240** PUBLICATIONS   **8,648** CITATIONS

# Effect of Mutation of Carboxyl Side-Chain Amino Acids Near the Heme on the Midpoint Potentials and Ligand Binding Constants of Nitrophorin 2 and Its NO, Histamine, and Imidazole Complexes

Robert E. Berry,* Maxim N. Shokhirev, Arthur Y. W. Ho, Fei Yang,
Tatiana K. Shokhireva, Hongjun Zhang, Andrzej Weichsel, William R. Montfort, and
F. Ann Walker*

*Department of Chemistry and Biochemistry, The University of Arizona, P.O. Box 210041,
Tucson, Arizona 85721-0041*

Received October 15, 2008; E-mail: berryr@email.arizona.edu; awalker@email.arizona.edu

***Abstract:*** Nitrophorins (NPs) are a group of NO-carrying heme proteins found in the saliva of a blood-sucking insect from tropical Central and South America, *Rhodnius prolixus*, the "kissing bug". NO is kept stable for long periods of time by binding it as an axial ligand to a ferriheme center. The fact that the nitrophorins are stabilized as $Fe^{III}$–NO proteins is a unique property because most heme proteins are readily autoreduced by excess NO and bind NO to the Fe(II) heme irreversibly ($K_d$s in the picomolar range). In contrast, the nitrophorins, as Fe(III) heme centers, have $K_d$s in the micromolar to nanomolar range and thus allow NO to dissociate upon dilution following injection into the tissues of the victim. This NO can cause vasodilation and thereby allow more blood to be transported to the site of the wound. We prepared 13 site-directed mutants of three major nitrophorins, NP2, NP1, and NP4, to investigate the stabilization of the ferric–NO heme center and preservation of reversible binding that facilitates these proteins' NO storage, transport, and release functions. Of the mutations in which Glu and/or Asp were replaced by Ala, most of these carboxyls show a significant role stabilizing $Fe^{III}$–NO over $Fe^{II}$–NO, with buried E53 of NP2 or E55 of NP1 and NP4 being the most important and partially buried D29 of NP2 or D30 of NP4 being second in importance. The p$K_a$s of the carboxyl groups studied vary significantly but all are largely deprotonated at pH 7.5 except E124.

## Introduction

The nitrophorins (nitro = NO, phorin = carrier) are a group of NO-carrying heme proteins found in the saliva of at least two species of blood-sucking insects, *Rhodnius prolixus*, the "kissing bug", which has four such proteins in the adult insect[1–6] and at least three additional nitrophorins in earlier stages of development,[7,8] and *Cimex lectularius*, the bedbug, which has only one.[9,10] These interesting heme proteins sequester nitric oxide that is produced by a nitric oxide synthase (NOS) that is similar to vertebrate constituitive NOS and is present in the cells of the salivary glands.[11,12] NO is kept stable in the salivary glands for long periods of time by binding it as an axial ligand to a ferriheme center.[1,3–6] Upon injection into the tissues of the victim NO dissociates (as a result of dilution by ~1/100 and a pH rise from ~5–5.5 to ~7.2–7.5[29]), diffuses through the tissues to the nearby capillaries to cause vasodilation, and thereby allow more blood to be transported to the site of the wound. At the same time, histamine, whose role is to cause swelling, itching, and initiation of the immune response, is released by mast cells and platelets of the victim. In the case of the *Rhodnius* proteins this histamine binds to the heme sites of the nitrophorins, hence preventing the insect's detection for a period of time.[13] These two properties of the nitrophorins of *Rhodnius prolixus* contribute to transmission of the protozoan

(1) Ribeiro, J. M. C.; Hazzard, J. M. H.; Nussenzveig, R.; Champagne, D.; Walker, F. A. *Science* **1993**, *260*, 539–541.

(2) Champagne, D. E.; Nussenzveig, R. H.; Ribeiro, J. M. C. *J. Biol. Chem.* **1995**, *270*, 8691–8695.

(3) Walker, F. A.; Ribeiro, J. M. C.; Montfort, W. R. In *Metal Ions in Biological Systems*; Sigel, H., Sigel A., Eds.; Marcel Dekker: New York, 1999; Vol. 36 (Interrelations between Free Radicals and Metal Ions in Life Processes), pp 619–661.

(4) Walker, F. A.; Montfort, W. R. In *Advances in Inorganic Chemistry*; Mauk, G., Sykes, A. G., Eds.; Academic Press: San Diego, 2001; Vol. 51, Chapter 5, pp 295–358.

(5) Walker, F. A. *J. Inorg. Biochem.* **2005**, *99*, 216–236.

(6) Walker, F. A. In *The Smallest Biomolecules: Diatomics and their Interactions with Heme Proteins*; Ghosh, A., Ed.; Elsevier B. V.: Amsterdam, 2008; pp 378–428.

(7) Moreira, M. F.; Coelho, H. S.; Zingali, R. B.; Oliveira, P. L.; Masuda, H. *Insect Biochem. Mol. Biol.* **2003**, *33*, 23–28.

(8) Andersen, J. F.; Gudderra, N.; Francischetti, I. M. B.; Valenzuela, J. G.; Ribeiro, J. M. C. *Biochemistry* **2004**, *43*, 6987–6994.

(9) Valenzuela, J. G.; Walker, F. A.; Ribeiro, J. M. C. *J. Exper. Biol.* **1995**, *198*, 1519–1526.

(10) Weichsel, A.; Maes, E. M.; Andersen, J. F.; Valenzuela, J. G.; Shokhireva, T. Kh.; Walker, F. A.; Montfort, W. R. *Proc. Natl. Acad. Sci. U.S.A.* **2005**, *102*, 594–599.

(11) Nussenzveig, R. H.; Bentley, D. L.; Ribeiro, J. M. C. *J. Exper. Biol.* **1995**, *198*, 1093–1098.

(12) Yuda, M.; Hirai, M.; Miura, K.; Matsumura, H.; Ando, K.; Chinzei, Y. *Eur. J. Biochem.* **1996**, *242*, 807–812.

(13) Ribeiro, J. M. C.; Walker, F. A. *J. Exper. Med.* **1994**, *180*, 2251–2257.

*Trypanasoma cruzi*, the vector of Chagas' disease,[14] to the victim via the feces of the insect that are left behind at the site of the bite[3] following the extended feeding time.

The *Rhodnius* proteins of the adult insect, which have been named NP1−4 in order of their abundances in the insect saliva, have been investigated by a number of techniques[1,3,6,15−37] including spectroelectrochemistry,[15,17−20] infrared[15] and resonance Raman,[16] NMR,[15,18,21−25] EPR[15,26] and Mössbauer spectroscopies,[27] and stopped-flow photometry,[17,28] and the solid-state structures of one or more ligand complexes of NP1,[15,29] NP2[30,31] and NP4[32−37] have been determined by X-ray crystallography. The structures are unique for heme proteins in that the heme is located at the open end of a $\beta$-barrel of the lipocalin fold[9,38] rather than in the more commonly observed largely α-helical globin or 4-helix bundle folds. The ferriheme molecule is bound to the protein via a histidine ligand, and the sixth coordination site is available to bind NO or other ligands. In the NO-off form in vitro, either water or ammonia, depending on buffer type, is bound to the sixth site.[29,32]

The fact that the nitrophorins are stabilized as ferriheme proteins is a unique property, for most heme proteins, including myoglobins and hemoglobins, are autoreduced by excess NO and bind NO to the Fe(II) heme with $K_d$s in the picomolar range,[39,40] which would make NO binding irreversible from the insect's point of view. In contrast, the nitrophorins, as Fe(III) heme centers, have $K_d$s in the micro- to nanomolar range and thus allow NO to dissociate under the concentration and pH conditions present in the tissues of the mammalian victim. While the pH of the insect salivary glands is believed to be between 5.0 and 5.5, the pH of the tissues of the mammalian victims is between 7.2 and 7.5, and earlier studies of the wild-type nitrophorins showed that the $K_d$s for NO dissociation range from 50 nM at pH 5.5 to 120 nM at pH 7.5 for NP4 and from 1 nM at pH 5.5 to 20 nM at pH 7.5 for NP2.[19]

Another way of saying that the nitrophorins are stabilized as ferriheme proteins is to point out that the midpoint potentials of the nitrophorins are approximately 300 mV more negative than those of met-myoglobins.[15] The work of Boxer, Gray, and co-workers showed that introduction of a Glu or Asp in the distal pocket of sperm whale myoglobin at the position of the distal valine E7 shifted the midpoint potential of that protein some 200 mV negative,[41] although at least the glutamate side chain was later shown by NMR spectroscopy to be actually bound to Fe.[42] We suspected that the Glu and Asp residues that are present near the heme center of the nitrophorins, all of which are far enough away that they cannot coordinate to Fe, might contribute to the negative midpoint potentials of these proteins. We thus prepared 13 site-directed mutants of the three major nitrophorins (1 lysine, 12 carboxyl (Asp or Glu) mutants) and investigated the $E_m$s of these mutant proteins over the pH range 5.5 to 7.5 for the ligand-free proteins as well as their NO complexes. The binding constants of NO, histamine and imidazole ligands to the ferric forms of the proteins over this pH range have also been determined. As will be seen, eight of the nine carboxyl groups studied, ranging in distance from 8 to 18.5 Å from the closest side-chain carboxyl oxygen to Fe, contribute to stabilizing Fe$^{III}$−NO with its nanomolar $K_d$s, over Fe$^{II}$−NO with its pico- to femtomolar $K_d$s.

Of the four major nitrophorins in the adult insects, the NP1 and NP4 pair is 90% identical in sequence, while NP2 and NP3 are 79% identical, with overall sequence identity being 45%. The genes for the four NPs of the adult insect each include a leader sequence designed for export of the proteins from the endothelial cells, where they are expressed, to the salivary glands, where the leader sequence is then cleaved. This cleavage leads to the native proteins found in the insect saliva having first residues K1, D1, D1, and A1 for NP1, NP2, NP3, and NP4, respectively. However, when the four "native" proteins are produced recombinantly from the truncated genes only NP4 is found to have its native A1 as the first residue; the other three have the M0 that results from the start codon of the gene still being present because the *E. coli* methionine aminopeptidase cannot cleave M0 if it is followed by an amino acid with a charged side chain. Therefore, the N-terminal sequences of these three are in actuality NP1-M0K1, NP2-M0D1, and NP3-M0D1.

(14) Kirchhoff, L. V. *N. Engl. J. Med* **1993**, *329*, 639–644.
(15) Ding, X. D.; Weichsel, A.; Andersen, J. F.; Shokhireva, T. Kh.; Balfour, C.; Pierik, A. J.; Averill, B. A.; Montfort, W. R.; Walker, F. A. *J. Am. Chem. Soc.* **1999**, *121*, 128–138.
(16) Maes, E. M.; Walker, F. A.; Montfort, W. R.; Czernuszewicz, R. S. *J. Am. Chem. Soc.* **2001**, *123*, 11664–11672.
(17) Andersen, J. F.; Ding, X. D.; Balfour, C.; Champagne, D. E.; Walker, F. A.; Montfort, W. R. *Biochemistry* **2000**, *39*, 10118–10131.
(18) Shokhireva, T. Kh.; Berry, R. E.; Uno, E.; Balfour, C. A.; Zhang, H.; Walker, F. A. *Proc. Natl. Acad. Sci. U.S.A.* **2003**, *100*, 3778–3783.
(19) Berry, R. E.; Ding, X. D.; Shokhireva, T. Kh.; Weichsel, A.; Montfort, W. R.; Walker, F. A. *J. Biol. Inorg. Chem* **2004**, *9*, 135–144.
(20) Berry, R. E.; Shokhireva, T. Kh.; Filippov, I.; Shokhirev, M. N.; Zhang, H.; Walker, F. A. *Biochemistry* **2007**, *46*, 6830–6843.
(21) Shokhireva, T. Kh.; Shokhirev, N. V.; Walker, F. A. *Biochemistry* **2003**, *42*, 679–693.
(22) Shokhireva, T. Kh.; Smith, K. M.; Berry, R. E.; Shokhirev, N. V.; Balfour, C. A.; Zhang, H.; Walker, F. A. *Inorg. Chem.* **2007**, *46*, 170–178.
(23) Shokhireva, T. Kh.; Weichsel, A.; Smith, K. M.; Berry, R. E.; Shokhirev, N. V.; Balfour, C.; Zhang, H.; Montfort, W. R.; Walker, F. A. *Inorg. Chem.* **2007**, *46*, 2041–2056.
(24) Shokhireva, T. Kh.; Berry, R. E.; Zhang, H.; Shokhirev, N. V.; Walker, F. A. *Inorg. Chim. Acta* **2008**, *361*, 925–940.
(25) Shokhireva, T. Kh.; Shokhirev, N. V.; Berry, R. E.; Zhang, H.; Walker, F. A. *J. Biol. Inorg. Chem.* **2008**, *13*, 941–959.
(26) Astashkin, A. V.; Raitsimring, A. M.; Walker, F. A. *Chem. Phys. Lett.* **1999**, *306*, 9–17.
(27) Wegner, P.; Benda, R.; Schünemann, V.; Trautwein, A. X.; Berry, R. E.; Balfour, C. A.; Wert, D.; Walker, F. A. *Hyperfine Interact. C* **2002**, *5*, 253–256.
(28) Andersen, J. F.; Champagne, D. E.; Weichsel, A.; Ribeiro, J. M. C.; Balfour, C. A.; Dress, V.; Montfort, W. R. *Biochemistry* **1997**, *36*, 4423–4428.
(29) Weichsel, A.; Andersen, J. F.; Champagne, D. E.; Walker, F. A.; Montfort, W. R. *Nat. Struct. Biol.* **1998**, *5*, 304–309.
(30) Andersen, J. F.; Montfort, W. R. *J. Biol. Chem.* **2000**, *275*, 30496–30503.
(31) PDB files available (http://www.rcsb.org/): 1PEE, 1PM1, 1T68, 2A3F, 2ACP, 2AH7, 2AL0, 2ALL, 2AMM, 2ASN, 2EU7, 2HYS, 2GTF. Weichsel, A.; Berry, R. E.; Zhang, H.; Walker, F. A.; Montfort, W. R.
(32) Andersen, J. F.; Weichsel, A.; Balfour, C. A.; Champagne, D. E.; Montfort, W. R. *Structure* **1998**, *6*, 1315–1327.
(33) Weichsel, A.; Andersen, J. F.; Roberts, S. A.; Montfort, W. R. *Nat. Struct. Biol.* **2000**, *7*, 551–554.
(34) Roberts, S. A.; Weichsel, A.; Qiu, Y.; Shelnutt, J. A.; Walker, F. A.; Montfort, W. R. *Biochemistry* **2001**, *40*, 11327–11337.
(35) Maes, E. M.; Weichsel, A.; Andersen, J. F.; Shepley, D.; Montfort, W. R. *Biochemistry* **2004**, *43*, 6679–6690.
(36) Kondrashov, D. A.; Roberts, S. A.; Weichsel, A.; Montfort, W. R. *Biochemistry* **2004**, *43*, 13637–13647.
(37) Maes, E. M.; Roberts, S. A.; Weichsel, A.; Montfort, W. R. *Biochemistry* **2005**, *44*, 12690–12699.
(38) Montfort, W. R.; Weichsel, A.; Andersen, J. F. *Biochim. Biophys. Acta* **2000**, *1482*, 110–118.

(39) Hoshino, M.; Ozawa, K.; Seki, H.; Ford, P. C. *J. Am. Chem. Soc.* **1993**, *115*, 9568–9575.
(40) Lim, M. D.; Lorcovic, I. M.; Ford, P. C. *J. Inorg. Biochem.* **2005**, *99*, 151–165.
(41) Varadarajan, R.; Zewert, T. E.; Gray, H. B.; Boxer, S. G. *Science* **1989**, *243*, 69–72.
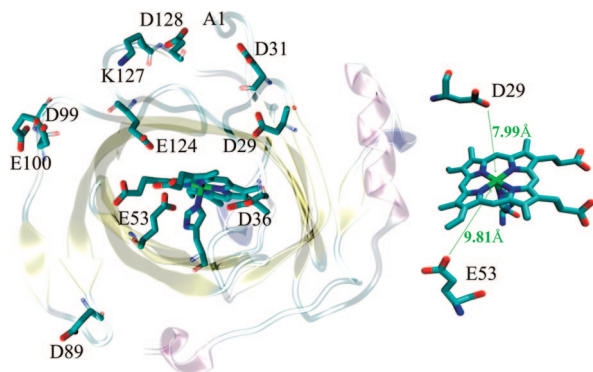(42) Zewert, T. E.; Gray, H. B.; Bertini, I. *J. Am. Chem. Soc.* **1994**, *116*, 1169–1173.

**Figure 1.** Ten residues mutated in this study and their relationship to the position of the heme inside the lipocalin β-barrel of NP2-D1A. The position of the A1 residue is also shown, and a closeup of the two buried residues, D29 and E53, is shown at the right. E55 of NP1 and NP4 and D30 of NP4 are at almost identical positions to E53 and D29 of NP2.

In this work we used the D1A mutant of NP2, which, like NP4, has M0 cleaved during expression, as standard (NP2-D1A) because of the finding that removal of the Met-0 resulting from the start codon has a marked effect on the kinetics of heme reorientation in the heme cavity, the equilibrium ratio of heme rotational isomers **A** and **B** for NO-free and ligand-bound complexes of NP2, and the rate of histamine binding and release.[20]

Ligand binding constants to the ferric and ferrous forms of the protein are related to the difference in midpoint potentials of the ligand-free and ligand-bound forms of the protein via the following equilibria

$$Fe^{III} + e^- \rightleftharpoons Fe^{II} \qquad E_m \qquad (1)$$

$$Fe^{III} + L \rightleftharpoons Fe^{III}-L \qquad K_f^{III} \qquad (2)$$

$$Fe^{II} + L \rightleftharpoons Fe^{II}-L \qquad K_f^{II} \qquad (3)$$

$$Fe^{III}-L + e^- \rightleftharpoons Fe^{II}-L \qquad E_{m,c} \qquad (4)$$

because the Nernst equation can be rewritten as

$$E_{m,c} - E_m = -(RT/nF)\ln(K_f^{III}/K_f^{II}) \qquad (5)$$

where as indicated in eqs 2 and 3 $K_f^{III}$ and $K_f^{II}$ are the binding constants for ligand L to the $Fe^{III}$ and $Fe^{II}$ states of the protein, respectively, $R$ is the universal gas constant, and $F$ is the Faraday constant.

Of the mutants prepared in the NP2-D1A construct, one has K mutated to A, eight have E or D mutated to A, and one has E mutated to Q (because the E53A mutant of NP2 would not fold). It should be noted that in all cases we *removed* potential charges rather than *introducing* them. Thus, the structure of the NP2-D1A(NH₃) complex (PDB file 2EU7) could be used to measure the distance between the potentially charged side chain and the Fe in the native protein. The locations of the single carboxyl groups in the NP2-D1A construct are shown in Figure 1. Of the nine sites at which carboxyl groups were replaced by an uncharged group, five are at positions that have carboxyls conserved among the four nitrophorins (not conserved are D36, D99,, E100, and E124), and all of the five conserved residues are shown to play significant roles in shifting the metal midpoint potential negative. However, several nonconserved residues also play significant roles. Of the conserved residues that play a significant role, the equivalent of E53 was also mutated in NP1

and NP4 (NP1-E55Q and NP4-E55Q, respectively) and the equivalent of the D29 residue of NP2 was mutated in NP4 (NP4-D30A).

In analyzing the altered midpoint potentials of the NP2 mutants prepared in this study we considered the effect of the charge of each of the ionizable residues on the free energy of the ferriheme center. We expect that at the pH of the tissues of the victim (7.2−7.5) most of the carboxyls of interest are ionized and some may be ionized at the pH of the salivary gland (5.0−5.5) depending on the carboxyl $pK_a$. Thus, wherever possible we measured the potentials at pH 5.5, 6.5, and 7.5 and utilized the changes in $E_m$ with pH to estimate the $pK_a$ value of each carboxyl at pH 7.5 by procedures that are discussed below.

To analyze the effect of these charged residues we must know something about the polarity of the protein medium in which they are found. Despite the extensive work in the field of protein dielectric screening, where numerous systems have been subjected to very careful and systematic study over the past 30 years,[43−70] the common belief of many is that the interior of a protein has a dielectric constant of 1−4, indicating an oil-drop sort of medium, and values such as these have been used by a number of researchers in the field.[56−67] However, as Warshel and co-workers have pointed out in numerous publications, the dielectric "constant" of a protein is not a simple number because it depends entirely on the property studied and the model

(43) Warshel, A.; Levitt, M. *J. Mol. Biol.* **1976**, *103*, 227–249.
(44) Warshel, A.; Russell, S. T.; Churg, A. K. *Proc. Natl. Acad. Sci. U.S.A.* **1984**, *81*, 4785–4789.
(45) Warshel, A.; Russell, S. T. *Q. Rev. Biophys.* **1984**, *17*, 283–422.
(46) Warshel, A. *Nature* **1987**, *330*, 15–16.
(47) Cutler, R. L.; Davies, A. M.; Creighton, S.; Warshel, A.; Moore, G. R.; Smith, M.; Mauk, A. G. *Biochemistry* **1989**, *28*, 3188–3197.
(48) Lee, F. S.; Chu, Z. T.; Warshel, A. *J. Comput. Chem.* **1993**, *14*, 161–185.
(49) Alden, R. G.; Parson, W. W.; Chu, Z. T.; Warshel, A. *J. Phys. Chem.* **1996**, *100*, 16761–16770.
(50) Muegge, I.; Qi, P. X.; Wand, A. J.; Chu, Z. T.; Warshel, A. *J. Phys. Chem. B* **1997**, *101*, 825–836.
(51) Sham, Y. Y.; Chu, Z. T.; Warshel, A. *J. Phys. Chem. B* **1997**, *101*, 4458–4472.
(52) Sham, Y. Y.; Muegge, I.; Warshel, A. *Biophys. J.* **1998**, *74*, 1744–1753.
(53) Schutz, C. N.; Warshel, A. *Proteins: Struct., Funct., Genet.* **2001**, *44*, 400–417.
(54) Johnson, E. T.; Parson, W. W. *Biochemistry* **2002**, *41*, 6483–6494.
(55) Warshel, A.; Sharma, P. K.; Kato, M.; Parson, W. W. *Biochim. Biophys. Acta* **2006**, *1764*, 1647–1676.
(56) Klapper, I.; Hagstrom, R.; Fine, R.; Sharp, K.; Honig, B. *Proteins: Struct., Funct., Genet.* **1986**, *1*, 47–59.
(57) Gilson, M. K.; Honig, B. *Nature* **1987**, *330*, 84–86.
(58) Gilson, M.; Sharp, K. A.; Honig, B. *J. Comput. Chem.* **1987**, *9*, 327–335.
(59) Nicholls, A.; Honig, B. *J. Comput. Chem.* **1991**, *12*, 435–445.
(60) Honig, B.; Nicholls, A. *Science* **1995**, *268*, 1144–1149.
(61) Sternberg, M. J. E.; Hayes, F. R. F.; Russell, A. J.; Thomas, P. G.; Fersht, A. R. *Nature* **1987**, *330*, 86–88.
(62) Loewenthal, R.; Sancho, J.; Reinikainen, T.; Fersht, A. R. *J. Mol. Biol.* **1993**, *232*, 574–583.
(63) Gunner, M. R.; Honig, B. *Proc. Natl. Acad. Sci. U.S.A.* **1992**, *88*, 9151–9155.
(64) Gunner, M. R.; Nicholls, A.; Honig, B. *J. Phys. Chem.* **1996**, *100*, 4277–4291.
(65) Alexov, E.; Gunner, M. R. *Biophys. J.* **1997**, *72*, 2075–2093.
(66) Alexov, E.; Miksovska, J.; Baciou, L.; Schiffer, M.; Hanson, D. K.; Sebban, P.; Gunner, M. R. *Biochemistry* **2000**, *39*, 5940–5952.
(67) Gunner, M. R.; Alexov, E. *Biochim. Biophys. Acta* **2000**, *1458*, 63–87.
(68) Dwyer, J. J.; Gittis, A. G.; Karp, D. A.; Lattman, E. E.; Spencer, D. S.; Stites, W. E.; Garcia-Moreno, E. B. *Biophys. J.* **2000**, *79*, 1610–1620.
(69) Kao, Y.-H.; Fitch, C. A.; Bhattacharya, S.; Sarkisian, C. J.; Lecomte, J. T. J.; Garcia-Moreno, E. B *Biophys. J.* **2000**, *79*, 1637–1654.
(70) Lee, K. K.; Fitch, C. A.; Lecomte, J. T. J.; Garcia-Moreno, E. B. *Biochemistry* **2000**, *41*, 5656–5667.

used.[43−55] For calculations of charge stabilization by the protein environment (without ionized groups) semimacroscopic models with an adjustable protein dielectric constant $\varepsilon_p$ and a water dielectric $\varepsilon_w$ of 78.5, have been used, as in the Poisson−Boltzmann (PB) model, or the more quantitative semimicroscopic Protein Dipole Langevin−Dipole linear response approximation (PDLD/S-LRA) method[48,50−52] has been used, in which the same parameters have been fit to the data of individual studies. However, it has been pointed out repeatedly that $\varepsilon_p$ does not represent the actual "dielectric constant" of the protein but rather a scaling factor that represents the contributions that are not treated explicitly in the particular model.[52] In treatments that explicitly consider protein reorganization $\varepsilon_p$ is between 4 and 6 as in the case of cytochrome *c* discussed by Muegge et al.[50] However, if the calculations do not allow for protein reorganization during the charging process $\varepsilon_p$ may need to be set as high as 40.[50] The bulk dielectric constant, $\bar{\varepsilon}$, that reflects the response of the protein to external field is very different from $\varepsilon_p$ and is not useful for analysis of redox properties.[50,55]

In contrast, an effective dielectric constant, $\varepsilon_{eff}$, can be defined for charge−charge interactions (which represents the effect of $\varepsilon_p$, the effect of the protein reorganization, and the effect of the solvent). This $\varepsilon_{eff}$ predicts basically a Coulomb's law dependence of the free energy of interaction between charged centers *i* and *j* with charges $q_i$ and $q_j$ separated by a distance $r_{ij}$[44,53]

$$\Delta G_{ij} = -1389 q_i q_j / \varepsilon_{eff} r_{ij} (\text{in kJ/mol}) \ (= -nF\Delta E_m \text{ in our case})$$
(6)

The value of $\varepsilon_{eff}$ is usually approximated by a large number, often between 20 and 40 (or up to 80), or by a distance-dependent function.[44,53,54]

A number of studies of the effect of charged groups on the midpoint potential $E_m$ at physiological pH, of the iron in a heme protein,[41,47,71−75] or of the special pair of chlorophylls in bacterial reaction centers[54,76] have been reported. In most of these cases the authors had very specific goals in mind, and thus, little or no attempt was made to determine whether such distance dependence is observed for cases where the heme or special pair is buried within the protein and the charged groups are either buried, partially buried, or exposed to the aqueous medium. However, Johnson and Parson carefully treated the $E_m$ values of their Reaction Center mutants; they found that the dielectric is large even at small distances, and thus, any model with large dielectric constant works much better than all macroscopic models that use a small dielectric.[54] In the present case, of the 10 carboxyl or lysine mutants of NP2 shown in Figure 1 we found that most of them behave according to eq 6 with some scatter with the appropriate value of $\varepsilon_{eff}$ being about 15. However, the fit is significantly improved when the charged

groups' fractional protonation states (based on the estimated $pK_a$ of each group) are taken into account, as will be discussed below.

## Experimental Section

**Protein Sample Preparation.** Standard genetic engineering methods were employed to produce the various target nitrophorin gene mutants in the pET24a or pET17b (Novagen) expression plasmids and confirmed by sequencing. The *E. coli*-expressed proteins were purified as described elsewhere[18,20] and preliminarily characterized by UV−visible, NMR, and EPR spectroscopy and mass spectrometry using MALDI-TOF (matrix-assisted laser desorption time-of-flight) and/or electrospray. The purified proteins were stored in lyophilized form at −80 °C until use.

**Spectroscopic Characterization of the NPs and Their Mutants.** The NP2-D1A parent of the NP2-D1A, second carboxyl mutants of this study has been fully characterized by MALDI-TOF, UV−vis, spectroelectrochemistry, 1D and 2D ¹H and ¹³C NMR spectroscopy, and stopped-flow kinetics as described in detail elsewhere.[20] Wild-type NP1[15] and NP4[17,32,37] UV−vis and heme substituent NMR[22,23] spectra and the structure of the NO complex of the NP4-D30A mutant[35] have been published previously. Sample UV−vis spectra of NP2-D1A, second carboxyl or amine mutants are shown in Figures 2, 5, and 6 and the same as for the NP2-D1A parent[20] and for wt NP2, also known as NP2-M0D1,[17−20] published elsewhere; all other NP2-D1A, second carboxyl or amine mutants had identical UV−vis spectra to those shown in Figures 2, 5, and 6, except for the ferrous form of NP2-D1A,D29A when bound to NO, the latter of which is discussed in the text below. The Soret band maxima of ferric NO-bound NP2-D1A and all of its mutants were observed at about 422 and 424 nm at pH 7.5 and 5.5, respectively, as shown in Supporting Information Table S5. Similarly, the Soret band maxima of the ferric NO complexes of NP1, NP4, and their mutants were at 418 and 420 nm at pH 7.5 and 5.5, respectively. As discussed previously,[19] the *ferrous* NO-bound nitrophorins were typical of either six-coordinate (∼416 nm) or five-coordinate heme−NO centers (∼398 nm), the latter of which was due to breakage of the proximal histidine−iron bond. The NO complexes of ferrous NP1 and NP4 are six coordinate at both pH values, and NP2 is six coordinate at pH 7.5 and five coordinate at pH 5.5 (in the ferrous NO-bound form).[19] The Soret band maxima of ferrous NO-bound mutants were the same as the wild-type Soret band maxima with some exceptions. NP4-D30A and the equivalent NP2-D1A,D29A mutant appeared to be mostly five-coordinate at both pH values, and to a lesser extent this is also the case for NP2-D1A,D36A and NP2-D1A,D89A. Conversely, NP2-D1A,E53Q appears to be mostly six coordinate at both pH values with a shoulder at ∼400 nm at pH 5.5 that indicates some fraction to be five coordinate.

EPR spectra of the imidazole complexes of wt NP4,[19] the histamine complex of NP2,[26] and the cyanide complex of NP4[23] have been published, and those of the same ligand complexes of the wild-type and mutant NPs of this study were identical to the published spectra. 1D ¹H NMR spectra of the imidazole complexes of all but one of the NP2-D1A, second carboxyl and amine mutant proteins of this study, as well as NP1-E55Q and NP4-E55Q and -D30A are provided in the Supporting Information, NMR Spectra S1−S5, which clearly show that the double mutation of D1 and another residue to A (or Q) do not affect the pattern of heme resonances, except for those of NP2-D1A,E53Q, NP1-E55Q, and NP4-E55Q. The NP2-D1A, second carboxyl mutant whose ¹H NMR spectrum is not presented in the Supporting Information is that of NP2-D1A,D89A; none of the mutant protein was left following electrochemical and binding constant measurements. However, the similarity of the NMR spectra of the other mutants and the distance of D89 from Fe both suggest that this mutant would not have an anomalous ¹H NMR spectrum. More extensive NMR data, including 2D NMR data showing chemical exchange cross peaks, on the E→Q

(71) Worrall, J. A. R.; Schlarb-Ridley, B. G.; Reda, T.; Marcaida, M. J.; Moorlen, R. J.; Wasti, J.; Hirst, J.; Bendall, D. S.; Luisi, B. F.; Howe, C. J. *J. Am. Chem. Soc.* **2007**, *129*, 9468–9475.
(72) Efimov, I.; Papadopoulou, N. D.; McLean, K. J.; Badyal, S. K.; Macdonald, I. K.; Munro, A. W.; Moody, P. C. E.; Raven, E. L. *Biochemistry* **2007**, *46*, 8017–8023.
(73) Louro, R. O.; Catarino, T.; Paquete, C. M.; Turner, D. L. *FEBS Lett.* **2004**, *576*, 77–80.
(74) De la Cerda, B.; Diaz-Quintana, A.; Navarro, J. A.; Hervás, M.; De la Rosa, M. A. *J. Biol. Chem.* **1999**, *274*, 13292–13297.
(75) Crofts, A.; Hacker, B.; Barquera, B.; Yun, C-H.; Gennis, R. *Biochim. Biophys. Acta* **1992**, *1101*, 162–165.
(76) Williams, J. C.; Haffia, A. L. M.; McCulley, J. L.; Woodbury, N. W.; Allen, J. P. *Biochemistry* **2001**, *40*, 15403–15407.

mutants of NP1, NP2-D1A, and NP4 will be discussed elsewhere in the near future.

**Spectroelectrochemical Measurements.** Protein solutions (~0.05 mM) for electrochemical studies were prepared as described previously in 0.1 M sodium phosphate or sodium acetate buffer at the appropriate pH; 1 mM methyl viologen, 0.2 mM anthraquinone-2-sulfonate, 0.2 mM $Ru(NH_3)_6Cl_3$, and 1,1′-ferrocenedicarboxylic acid (all from Aldrich) were added as electrochemical mediators.[15,17] Spectroelectrochemical measurements with NO coordinated also employed SNAP as the NO source.

Methods for spectroelectrochemical measurements utilized the same instrumentation and type of reference electrode (Ag/AgCl, $E_m = -205$ mV vs SHE) as described previously.[15,17−19] Since the ratio of oxidized to reduced forms of the nitrophorins is directly related to the absorbances of the optical spectra via Beer's law (assuming the extinction coefficients of the reduced and oxidized species are different at the chosen wavelength), the change in absorbance with respect to applied potential can be fit to the Nernst equation (eq 1) using the nonlinear least-squares fitting algorithm in the software Origin

$$E_{app} = E_m \text{ (or } E_{m,c}) + 2.303(RT/nF)\log_{10}([Ox]/[Red]) \quad (7)$$

where $E_{app}$ is the applied potential, $E_m$ (or $E_{m,c}$) is the midpoint potential determined from these data, and [Ox] and [Red] are the concentrations of the protein in the Fe(III) and Fe(II) states, respectively. The measurements are made in the presence of either no ligand ($E_m$) or a high enough concentration of ligand to ensure full complexation for both oxidation states ($E_{m,c}$). The temperature of the measurements was 27 ± 1 °C.

**Measurement of Ligand Binding Constants for the Fe(III) Nitrophorins.** Measurements of ligand binding constants to the ferriheme forms of the nitrophorins were carried out by utilizing solutions which contained 0.1 M sodium phosphate buffer at the chosen pH. For nitric oxide (NO) binding studies the solutions also contained cuprous chloride (Aldrich, ~2 mM) and were extensively degassed with argon (see below). Nitric oxide binding measurements were performed using aliquots of a 200 μM solution of *S*-nitroso-*N*-acetyl-D,L-penicillamine (SNAP, at 98% purity, obtained from World Precision Instruments) in ultrapure water (18 mΩ) containing EDTA (50 μM) and prepared freshly the day of use. SNAP is a fairly stable compound that decomposes stoichiometrically and rapidly in the presence of Cu(I) to generate NO and a disulfide product, allowing a much more accurate titration than that produced by working with gaseous NO.[77]

Binding constant measurements were carried out as described previously[19] by adding aliquots of the chosen axial ligand to 1−10 μM solutions of each nitrophorin at the desired pH (usually 7.5) and fitting the data to a mutually depleting model[19,78,79] using the software Origin to perform the nonlinear least-squares fit to the equation

$$\Delta A / \Delta A_{max} = \frac{(P_t + L_t + K_d^{III}) - \{[(P_t + L_t + K_d^{III})^2 - (4L_t P_t)]^{0.5}\}}{2P_t} \quad (8)$$

where $\Delta A$ is the change in absorbance at a given wavelength for a specific total ligand concentration $L_t$, $\Delta A_{max}$ is the change in absorbance of the fully complexed species at the same wavelength, $P_t$ is the total protein concentration, and $K_d^{III}$ (= $1/K_f^{III}$) is the ligand dissociation constant (M) for ligand L from the Fe(III) protein. The temperature of the measurements was 27 ± 1 °C.

**NP4-E55Q(NH₃) Crystal Structure.** Crystals of the E55Q mutant of NP4 grew from 2.8 M ammonium phosphate, 100 mM Tris·HCl pH 7.5 using the hanging-drop vapor diffusion method at room temperature. A plate-like crystal with a thickness of ~20 μm was transferred to 3.5 M ammonium phosphate pH 5.6, equilibrated at room temperature for 20 min, and flash-frozen in liquid nitrogen. Diffraction data were measured at 100 K on SSRL beam line 9-1 using a CCD Quantum 4 detector and processed with d*TREK[80] as implemented in the CrystalClear software package (Rigaku). The crystal was in space group *C2* with unit cell parameters $a = 70.4$ Å, $b = 42.8$ Å, $c = 53.1$ Å, and $\beta = 94.2°$. The structure was determined to 1.5 Å resolution using difference Fourier methodology and a wild-type NP4 structure as a starting model (PDB entry 1D2U[34]). Model building was accomplished with COOT[81] and refinement with REFMAC5 in the CCP4 program suite.[82] The final model yielded crystallographic and free *R* factors of 0.17 and 0.20 and displayed excellent geometry. All residues were observed in the final electron density maps, but residues 30−39 (the A−B loop) displayed high mobility. Structural figures were made with PyMOL[83] and Adobe Illustrator 9.0. Final statistics are shown in Supporting Information Table S6. Coordinates and structure factors have been deposited in the Protein Data Bank under entry 3FLL.

## Results and Discussion

**Nitrophorin Fe(III)/Fe(II) Midpoint Potentials for Carboxyl and Amine Side-Chain Mutants.** In Figure 2a is shown an example of the spectroscopic data collected during an electrochemical titration of the NO complex of NP2-D1A,D89A at pH 5.5, and the inset, Figure 2b, shows the fit to eq 7 obtained for these data. The value of the midpoint potential ($E_m$) obtained, $-51 \pm 1$ mV vs SHE, is presented in Table 1 along with the $E_m$ values of all of the other mutants in both the ligand-free ($H_2O$ bound) and the NO-bound forms. For each pH and NO-bound form in Table 1 is also listed the *change* in $E_m$ relative to its appropriate standard value (NP2-D1A for the NP2 mutants and measured values for wild-type NP1 (NP1-M0K1) and NP4 for their respective mutants)

$$\Delta E_m = E_m(\text{mutant}) - E_m(\text{standard}) \quad (9)$$

Thus, $\Delta E_m$ should be a measure of the contribution to the $E_m$ that results from removal of the mutated carboxyl or amine side chain. However, in our analysis of the data it became clear that the $E_m$ and $\Delta E_m$ values of the nitrophorin mutants in the absence of NO were strongly affected by water molecules in the distal heme pocket, including one that is bound to the iron.[31−37] These effects will be discussed in detail below. In the NO-bound mutants, however, where most if not all of the water molecules have been expelled from the distal heme pocket, as revealed by X-ray crystallography,[31−37] it was possible to better analyze and interpret the changes in $\Delta E_m$ for various mutants. Thus, if the $\Delta E_m$ for the NO-bound mutants at pH 7.5 are plotted against the distance of Fe to the closest O/N of the mutated carboxyl/amine side chain (using the crystal structure PDB file 2EU7 for NP2-D1A mutants and files 2NP1 and 1X8P for NP1 and NP4, respectively) we would expect to see basically a Coulomb's law dependence, eq 6, as shown in Figure 3.

From a single-molecule perspective each carboxyl or amine side chain in a nitrophorin protein molecule will be either ionized or neutral ($q_j = -1$ or 0) with no state between these

(77) Zhang, X.; Cardosa, L.; Broderick, M.; Fein, H.; Davies, I. R. *Electroanalysis* **2000**, *12*, 425–428.

(78) Murataliev, M. B.; Feyereisen, R. *Biochemistry* **2000**, *39*, 12699–12707.

(79) *Enzyme Kinetics*; Segel, I. H., Ed; Wiley-Interscience: New York, 1975; p 73.

(80) Pflugrath, J. W. *Acta Crystallogr.* **1999**, *D55*, 1718–1725.

(81) Emsley, P.; Cowtan, K. *Acta Crystallogr.* **2004**, *D60*, 2126–2132.

(82) Collaborative Computational Project, Number 4. *Acta Crystallogr.* **1994**, *D50*, 760–763.
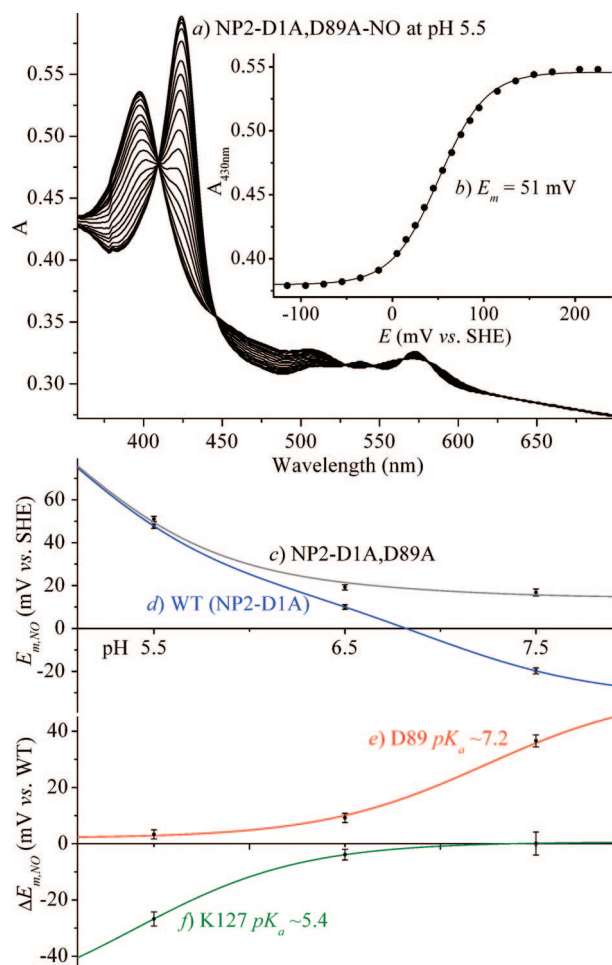
(83) DeLano, W. L., http://www.pymol.org.

**Figure 2.** (a) Spectroelectrochemical titration of the NO complex of NP2-D1A,D89A at pH 5.5 and 27 °C; (b) fit of the data to eq 7. (c) Determined $E_m$ value from the fit to these data at pH 5.5 (51 mV) is plotted along with the $E_m$ values at pH 6.5 and 7.5 for NP2-D1A,D89A(NO). (d) $E_m$ values for NP2-D1A(NO) against pH, and (e) change in $E_m$ for NP2-D1A,D89A(NO) relative to NP2-D1A ($\Delta E_m = E_{m(NP2-D1A,D89A)} - E_{m(NP2-D1A)}$), which is fit with a p$K_a$ of ~7.2 (in red). (f) Change in $E_m$ for NP2-D1A,K127A(NO) relative to NP2-D1A fit with a p$K_a$ of ~5.4 (in green).

two. Assuming $\varepsilon_{eff}$ and $r_{ij}$ are known, eq 6 should predict the effect of the carboxylate on $E_m$. Many of the mutants do indeed show a dependence using an effective dielectric constant ($\varepsilon_{eff}$) of ~20 or a distance-dependent exponential screening function[44,52−54]

$$\varepsilon_{eff}(r_{ij}) = 1 + E'[1 - \exp(-\mu r_{ij})] \quad (10)$$

where $E'$ is ~60, $\mu$ is 0.1 Å$^{-1}$, and the distance $r_{ij}$ is measured in Angstroms.[54] However, many show a significant deviation from the expected dependence (eq 6) and lie outside the region delineated by the dashed lines because $E_m$ is a thermodynamic property of an ensemble of nitrophorin molecules. Depending on a carboxyl group's p$K_a$, at any given pH a fraction $x$ of the molecules will have the carboxyl ionized while a fraction $1 - x$ will have it protonated. If the p$K_a$ were known then an effective $q_j$ could be determined and eq 6 would predict the effect of the carboxyl on $E_m$. Thus, some of the deviation in the dependence shown in Figure 3 can be attributed to a given carboxyl's not being completely ionized at pH 7.5 ($q_j$ smaller in magnitude than $-1$, depending on the residue's p$K_a$) and some because of involvement in structural changes (such as the D30 of NP4, which, in its protonated form, is involved in H-bonding interactions that form the 'closed loop' structure in the crystalline state).[35] In the NO complex of the D30A (and D30N) mutant
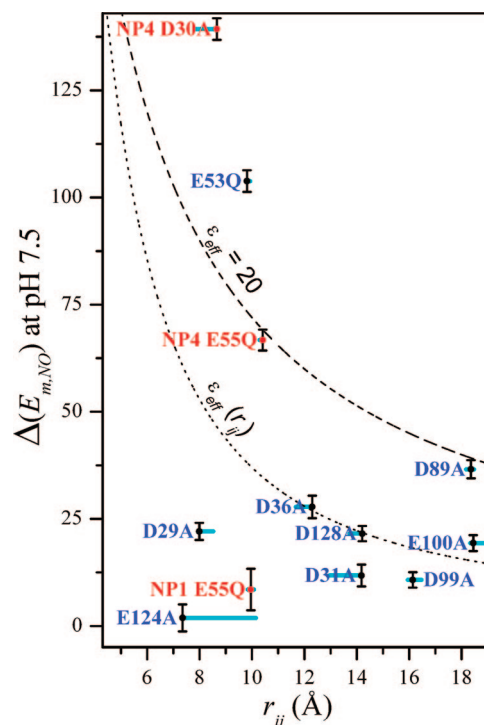


**Figure 3.** $\Delta E_m$ ($E_{m,(mutant)} - E_{m,(standard)}$) for the NO-bound mutants of the NPs at pH 7.5 plotted against the distance of Fe to the closest O atom of the mutated carboxyl side chain or the N of the mutated amino side chain (using the NP2-D1A crystal structure, PDB file 2EU7, NP1, file 2NP1 (distance used is the average of the two molecules in the unit cell), NP4, file 1X8P) with NP2-D1A mutants in blue and NP1 and NP4 mutants in red. These distances are from the 'best' crystal structures selected; other structures could have been used but did not have the ideal crystal form or resolution. These are shown by the horizontal line in cyan to represent the divergence in the distance of Fe to closest O in the other crystal structures (Supporting Information Table S4), PDB file 1EUO and 2A3F (NP2 structure at pH 7.7 and 6.5, respectively), and 1X8Q (NP4 structure at pH 5.6 (1X8P is at pH 7.4)), and for NP1 the two distances in each of the two molecules in the unit cell of PDB file 2NP1. The dashed lines represent the boundaries of the region covered for eq 6 by the distance-dependent effective dielectric constant of Schutz and Warshel, $\varepsilon_{eff}(r_{ij})$,[53] which is given by eq 10,[52−54] and an effective dielectric constant $\varepsilon_{eff} = 20$.

of NP4 a water molecule partially replaces the missing D30 carboxyl to form H bonds to D32 and D35. However, the fact that both of these mutant structures were solved at pH 5.6 and that both crystals photoreduced to the ferrous−NO complexes during structure determination[35] clouds somewhat our understanding of the effect of the loss of the carboxyl side chain on the observed structures, although it is unlikely that there could be major changes in the loop arrangements in the frozen state (100 K).

The spectroelectrochemical titration shown in Figure 2a is typical for NP2 and NP3 at pH 5.5 with a Soret band at ~398 nm when reduced with NO bound, presumably due to breakage of the proximal histidine−iron bond (five-coordinate ferrous heme−NO center).[17] At pH 7.5 the maximum shifts to ~416 nm (six-coordinate ferrous heme−NO center, Fe−N(His) bond length only 0.1 Å longer than for ferric heme−NO[37]) when reduced, whereas the maximum for the mutant NP2-D1A,D29A remains at ~398 nm even when reduced at pH 7.5, which indicates that the proximal histidine−iron bond that is normally present at pH 7.5 is broken in the D29A mutant at all pH values studied. The proximal histidine−iron bond in NP4 and M0-containing NP1 is stable at all pH values when reduced with NO bound ($\lambda_{max} \approx 416$ nm at pH 5.5−7.5), but the equivalent NP4-D30A mutant has a less stable proximal histidine−iron

***Table 1.*** Midpoint Potentials for Nitrophorins and Their Charge Mutants[a]

| | pH | $E_m$ | $\Delta(E_m)$[b] | $E_{m,NO}$ | $\Delta(E_{m,NO})$[b] | ref |
|---|---|---|---|---|---|---|
| NP1 | 5.5 | $-274 \pm 2$ | standard | $154 \pm 5$ | standard | 15 |
| | 6.5 | | standard | $118 \pm 3$ | standard | TW |
| | 7.5 | $-303 \pm 4$ | standard | $127 \pm 4$ | standard | 15 |
| NP2-D1A | 5.5 | $-318 \pm 1$ | standard | $48 \pm 1$ | standard | 20 |
| | 6.5 | $-327 \pm 6$ | standard | $10 \pm 1$ | standard | 20 |
| | 7.5 | $-325 \pm 3$ | standard | $-20 \pm 1$ | standard | 20 |
| NP4 | 5.5 | $-259 \pm 2$ | standard | $94 \pm 5$ | standard | 15 |
| | 6.5 | | standard | $44 \pm 2$ | standard | TW |
| | 7.5 | $-278 \pm 4$ | standard | $59 \pm 2$ | standard | 15,TW |
| NP2-D1A,<u>D29A</u> | 5.5 | $-334 \pm 3$ | $-17 \pm 3$ | $20 \pm 1$ | $-28 \pm 2$ | TW |
| | 6.5 | $-308 \pm 3$ | $19 \pm 6$ | $36 \pm 1$ | $26 \pm 2$ | TW |
| | 7.5 | $-313 \pm 1$ | $12 \pm 3$ | $2 \pm 1$ | $22 \pm 2$ | TW |
| NP4-<u>D30A</u> | 5.5 | $-213 \pm 1$ | $46 \pm 2$ | $181 \pm 2$ | $87 \pm 5$ | TW |
| | 6.5 | | | $163 \pm 4$ | $119 \pm 5$ | TW |
| | 7.5 | $-216 \pm 2$ | $62 \pm 4$ | $198 \pm 1$ | $139 \pm 2$ | TW |
| NP2-D1A,<u>D31A</u> | 5.5 | $-373 \pm 6$ | $-55 \pm 6$ | $38 \pm 2$ | $-10 \pm 2$ | TW |
| | 6.5 | $-372 \pm 8$ | $-45 \pm 9$ | $7 \pm 2$ | $-3 \pm 2$ | TW |
| | 7.5 | $-366 \pm 3$ | $-41 \pm 4$ | $-8 \pm 2$ | $12 \pm 3$ | TW |
| NP2-D1A,D36A | 5.5 | $-293 \pm 3$ | $25 \pm 4$ | $36 \pm 4$ | $-12 \pm 4$ | TW |
| | 6.5 | $-315 \pm 4$ | $11 \pm 7$ | $30 \pm 2$ | $20 \pm 2$ | TW |
| | 7.5 | $-307 \pm 4$ | $18 \pm 5$ | $8 \pm 2$ | $28 \pm 3$ | TW |
| NP1-<u>E55Q</u> | 5.5 | $-203 \pm 2$ | $115 \pm 3$ | $99 \pm 2$ | $-55 \pm 6$ | TW |
| | 6.5 | | | $119 \pm 6$ | $1 \pm 7$ | TW |
| | 7.5 | $-228 \pm 3$ | $97 \pm 5$ | $136 \pm 3$ | $9 \pm 5$ | TW |
| NP2-D1A,<u>E53Q</u> | 5.5 | $c$ | | $88 \pm 3$ | $40 \pm 3$ | TW |
| | 6.5 | $c$ | | $105 \pm 1$ | $95 \pm 2$ | TW |
| | 7.5 | $-316 \pm 3$ | $10 \pm 4$ | $84 \pm 2$ | $104 \pm 3$ | TW |
| NP4-<u>E55Q</u> | 5.5 | $-191 \pm 3$ | $68 \pm 3$ | $88 \pm 1$ | $-6 \pm 5$ | TW |
| | 6.5 | | | $67 \pm 2$ | $23 \pm 3$ | TW |
| | 7.5 | $-196 \pm 2$ | $82 \pm 4$ | $126 \pm 2$ | $67 \pm 2$ | TW |
| NP2-D1A,<u>D89A</u> | 5.5 | $-284 \pm 3$ | $34 \pm 3$ | $51 \pm 1$ | $3 \pm 2$ | TW |
| | 6.5 | $-304 \pm 4$ | $23 \pm 7$ | $19 \pm 1$ | $9 \pm 2$ | TW |
| | 7.5 | $-320 \pm 3$ | $5 \pm 4$ | $17 \pm 2$ | $37 \pm 2$ | TW |
| NP2-D1A,D99A | 5.5 | $-304 \pm 4$ | $14 \pm 4$ | $38 \pm 1$ | $-10 \pm 2$ | TW |
| | 6.5 | $-314 \pm 1$ | $13 \pm 6$ | $9 \pm 2$ | $-1 \pm 3$ | TW |
| | 7.5 | $-337 \pm 4$ | $-12 \pm 5$ | $-9 \pm 1$ | $11 \pm 2$ | TW |
| NP2-D1A,E100A | 5.5 | $-312 \pm 6$ | $6 \pm 6$ | $43 \pm 2$ | $-5 \pm 2$ | TW |
| | 6.5 | $-310 \pm 3$ | $17 \pm 7$ | $5 \pm 1$ | $-5 \pm 2$ | TW |
| | 7.5 | $-357 \pm 5$ | $-32 \pm 6$ | $0 \pm 1$ | $19 \pm 2$ | TW |
| NP2-D1A,E124A | 5.5 | $-193 \pm 4$ | $125 \pm 4$ | $52 \pm 5$ | $4 \pm 5$ | TW |
| | 7.5 | $-318 \pm 2$ | $7 \pm 4$ | $-18 \pm 3$ | $2 \pm 3$ | TW |
| NP2-D1A,<u>K127A</u> | 5.5 | $-327 \pm 5$ | $-9 \pm 5$ | $21 \pm 2$ | $-27 \pm 3$ | TW |
| | 6.5 | $-329 \pm 3$ | $-2 \pm 6$ | $6 \pm 2$ | $-4 \pm 2$ | TW |
| | 7.5 | $-379 \pm 2$ | $-54 \pm 4$ | $-20 \pm 4$ | $0 \pm 4$ | TW |
| NP2-D1A,<u>D128A</u> | 5.5 | $-311 \pm 4$ | $7 \pm 4$ | $32 \pm 3$ | $-16 \pm 4$ | TW |
| | 6.5 | | | $2 \pm 1$ | $-8 \pm 2$ | TW |
| | 7.5 | $-382 \pm 3$ | $-57 \pm 4$ | $2 \pm 1$ | $22 \pm 2$ | TW |

[a] Midpoint potentials in millivolts vs SHE; measured at 27 °C; conserved amino acids underlined. [b] $\Delta E_m = E_m(\text{mutant}) - E_m(\text{standard})$. [c] Not stable at low pH without NO bound. TW: This work.

bond ($\lambda_{\max} \approx 405$ nm at pH 5.5−7.5). Destabilization of the proximal histidine−iron bond in some mutants when reduced (with NO bound) is also likely to affect $E_m$ and contribute to some of the deviations in the dependence shown in Figure 3.

Three of the four carboxyl side chains closest to Fe in NP2, i.e., D29, D31, and D36, all of which are in the A−B loop, have conformations and distances from Fe that vary significantly depending on whether the loop is in the open or closed conformation.[31,35−37] For recombinant NP2 (M0-containing NP2) the loop is in the open conformation, D29 is farther from Fe than in the two NP2-D1A (M0 cleaved) structures (8.52 Å as compared to 7.99 and 8.00 Å), D31 is closer in M0-containing NP2 than in the two NP2-D1A structures (12.95 Å as compared to 14.18 and 14.19 Å), D36 is slightly closer in M0-containing NP2 than in the two D1A structures (12.18 Å as compared to 12.30 and 12.40 Å (PDB files 1EUO as compared to 2EU7 and 2ASN, respectively, in each case)).[31] The D36 carboxyl side chain is very much on the surface of the protein with its

$COO^-$ forming a hydrogen bond or salt bridge to $K62-NH_3^+$ in the pH 7.7 NP2-D1A($NH_3$) complex structure (2.64 Å, PDB file 2EU7) and in the pH 7.7 M0-containing NP2($NH_3$) complex (2.89 Å, PDB file 1EUO) and the pH 6.5 NP2-D1A imidazole complex (2.74 Å, PDB file 1PEE), and one pH 6.5 M0-containing NP2−Fe$^{II}$($H_2O$) complex (2.91 Å, PDB file 2AL0) but is somewhat farther away for the pH 6.5 M0-containing NP2−Fe$^{III}$($H_2O$) structure (3.33 Å, PDB file 2AH7) and considerably farther removed in the pH 7.5 M0-containing NP2−Fe$^{II}$(NO), the other pH 6.5 M0-containing NP2−Fe$^{III}$($H_2O$), and the other pH 6.5 M0-containing NP2−Fe$^{II}$($H_2O$) complexes (3.71, 3.71, and 4.00 Å, respectively, PDB files 1T68, 2A3F, and 2ACP, respectively).[31]

These structures represent two different crystal forms, with 2EU7, 1EUO, 1T68, 2A3F, and 2ACP having unit cells $P2_12_12$ (orthorhombic) and 1PEE, 2AH7, and 2AL0 having a unit cell $P4_12_12$ (tetragonal),[31] and thus, the good hydrogen-bond between the D36 carboxylate and K62 ammonium side chains is not

limited to one crystal form. Because K62 is on the surface of the protein it should be able to move freely, and thus, it is likely that this hydrogen bond or salt bridge exists in homogeneous solution. In the salt bridge the positive charge on K62 and the negative charge on D36 would cancel each other, producing no net charge or contribution to the $E_m$. Removal of the carboxylate, as in the D36A mutant, will likely leave K62 as a positively charged side chain; thus, the mutation in this case results in addition of a positive charge rather than removal of a negative one. The overall change in $E_m$ caused by this mutation will be equivalent to one in which a negative charge is removed since *addition* of a positive charge in approximately the same position will have the same destabilizing effect on the charge at Fe(III) as *removing* a negative charge (assuming the K62 positively charged side chain does not change position significantly in the mutant).

Another loop that has different conformations in various crystal structures is the G−H loop,[31] of which we have mutated K127 and D128. K127 does not interact with any other side chains in the M0-containing NP2 structures, but in both NP2-D1A structures it appears that K127 could interact with E124 without much readjustment of side chains (E124 of NP2 and NP3 is K125 in NP1 and NP4, and thus, the same interaction is not possible in those cases). Also, in one NP4 crystal structure (PDB file 1D2U) the equivalent K128 amine group is only 2.8 Å from a heme carboxylate and clearly forming a hydrogen bond that could affect the midpoint potential; likewise, K125 of NP4 also forms a hydrogen bond to a heme carboxylate which could affect the midpoint potential. We did not mutate either K125 or K128 of NP4 in this study. K127(128) and D128(129) are both conserved amino acids among the four NPs, and thus, they are likely to be particularly important to the redox chemistry of the heme iron. The carboxyl of D128 is 13.3 Å from the heme edge and 14.2 Å from the iron: distance measurements from the structure of NP2-D1A, PDB file 2EU7, which is the structure of the Fe$^{III}$(NH$_3$) complex. The carboxylate of D128 makes a weak hydrogen bond with R123 N$_\varepsilon$−H (O−N = 3.18 Å) in this crystal structure. The distance from Fe again varies with values of 14.21, 14.40, and 13.72 (PDB files 2EU7, 2ASN, and 1EUO, respectively).

Of the other mutants, the carboxyl of E100 appears to be H-bonded to K84 (O−N = 2.54 Å), and in this case the distance from Fe also varies with values of 18.45, 19.87, and 18.86 Å (PDB files 2EU7, 2ASN, and 1EUO, respectively). The carboxyl of D99 has no H-bond distance less than 3.22 Å, indicating only very weak H bonding. Distances to Fe vary from 16.14, 16.47, and 15.48 Å (PDB files 2EU7, 2ASN, and 1EUO, respectively). The carboxyl of D89 has a H bond to K91 at 3.08 Å. The distances vary from 18.36, 18.17, and 18.38 Å (PDB files 2EU7, 2ASN, and 1EUO, respectively). Some of the scatter in Figure 3 for these carboxyls can thus be attributed to somewhat variable distances between carboxylate charge and Fe.

Water molecules close to the heme iron may also contribute significantly to the value of $E_m$, and any mutations that change the positions of water molecules in the heme pocket may significantly alter the extent to which the positive charge on the iron is stabilized (independent of the charge mutated). Because there are a large number of crystal structures of NP2 (14) and NP4 (34) available in the protein databank we know that there are several water molecules near the heme iron of NP2 in the absence of NO or other added ligand, and one is even bound to the iron in the NO-off form at low pH (NH$_3$ is

bound at high pH). These water molecules may contribute to an increase in the polarity of the medium between the carboxyl and the iron, although their presence may not necessarily be responsible for the large $\varepsilon_{eff}$ (Figure 3), but rather, the large $\varepsilon_{eff}$ may reflect the reorientation of the protein polar groups. However, as nearly as we can determine, the orientation of NP2's E53 and NP4's E55 do not change in response to different numbers of waters near the heme. Another factor is that carboxyls located near the surface that are somewhat exposed to the aqueous medium still must interact with the buried heme iron positive charge in its somewhat polar environment. It is difficult to imagine a heme group, even in a membrane-bound protein such as the $bc_1$ complex of the respiratory chain, to be entirely free of water molecules, and the higher resolution structures now available of those protein complexes from various species do indeed show water molecules near the hemes, both hydrogen bonded to the propionate carboxylates and near the iron center, even though it has two axial histidine ligands.[84−91] With those structures now available, as well as some electrochemical data it would be interesting to see if high-level theoretical calculations of $\Delta E_m$ values would reproduce the measured $\Delta E_m$ values, and if so, under what conditions of $\varepsilon_{eff}$ and other relevant data. In that regard, it is interesting to note that the mutants of the photosynthetic reaction center of *Rhodobacter sphaeroides* prepared and studied by Johnson and Parson[54] required a high value of $\varepsilon_{eff}$ (or as it was called in their work, $\varepsilon_{in}$, = 20−40 depending on the model used) to match the measured $\Delta E_m$ values. They thus concluded that the electrostatic interactions of the special pair of chlorophylls, P/P$^+$, with ionizable amino acid residues are strongly screened and that this suggests that counterions make major contributions to this screening.[54] They found that the dielectric is large even at small distances, and thus, any model with a large dielectric constant, and in particular the distance-dependent $\varepsilon_{eff}(r_{ij})$ (eq 10), works much better than all macroscopic models with a small dielectric constant.[54]

A difficulty for all of the data presented in Figure 3 is that a Coulomb's law dependence should not be used to rationalize the effects on $E_m$ if it is measured at only one pH value, since it is likely that the residues in question are neither completely protonated nor completely deprotonated at the chosen pH. This is especially apparent for NP2-D1A,E53Q which shows a large $\Delta E_m$ at pH 7.5, close to what would be expected for a charge of −1 on the carboxylate (Figure 3). In contrast, the mutation of the equivalent conserved residue in NP1 (NP1-E55Q) shows an almost negligible $\Delta E_m$ (104 and 9 mV at pH 7.5 with NO bound, respectively). More will be discussed below about E53/ E55 and also D29/30, which present similar problems. For the moment, we see that measurements at only one pH value are

(84) Hunte, C.; Koepke, J.; Lange, C.; Rossmanith, T.; Michel, H. *Structure* **2000**, *8*, 669–684.
(85) Zhang, Z.; Huang, L.; Shulmeister, V. M.; Chi, Y.-I.; Kim, K. K.; Hung, L.-W.; Crofts, A. R.; Berry, E. A.; Kim, S.-H. *Nature* **1998**, *392*, 677–684.
(86) Berry, E. A.; Huang, L-S.; Zhang, Z.; Kim, S-H. *J. Bioenerg. Biomem.* **1999**, *31*, 177–190.
(87) Lange, C.; Nett, J. H.; Trumpower, B. L.; Hunte, C. *EMBO J.* **2001**, *20*, 6591–6600.
(88) Gao, X.; Wen, X.; Yu, C.-A.; Esser, L.; Tsao, S.; Quinn, B.; Zhang, L.; Yu, L.; Xia, D. *Biochemistry* **2002**, *41*, 11692–11702.
(89) Gao, X.; Wen, X.; Esser, L.; Quinn, B.; Yu, L.; Yu, C.-A.; Xia, D. *Biochemistry* **2003**, *42*, 9067–9080.
(90) Palsdottir, H.; Lojero, C. G.; Trumpower, B. L.; Hunte, C. *J. Biol. Chem.* **2003**, *278*, 31303–31311.
(91) Huang, L.; Cobessi, D.; Tung, E. Y.; Berry, E. A. *J. Mol. Biol.* **2005**, *351*, 573–597.

not sufficient to determine the effect of mutation of a potentially charged residue on the $E_m$ of the redox-active site of a protein. For this reason, we have not attempted to analyze $E_m$ data from other protein systems, which in general have been measured at only one pH value.[41,47,54,71-76]

**Interpretation of the Effect of pH on the Midpoint Potentials of the Carboxyl Mutants of the NO-Free and NO-Bound Nitrophorins.** The $E_m$ values of the nitrophorins vary with pH with significant, yet interpretable, changes being observed for the NO-bound $E_m$s, which decrease by as much as 68 mV between pH 5.5 and 7.5 (for the NO complex of NP2-D1A). This is likely because of the change in charge of ionizable residues as well as other structural changes that may occur between low and neutral pH (which are also likely to be triggered by the ionization of these residues). Since the functions of the nitrophorins are to store NO at low pH in the salivary gland and release NO at physiological pH in the victim while protecting the Fe$^{III}$−NO from reductive nitrosylation,[3-6] it is important to understand the residues that contribute to this function. Some ionizable carboxyl residues will be negatively charged to some extent at both physiological pH values and so contribute to the very negative $E_m$ of the nitrophorins and thus to the nitrophorin's resistance to reductive nitrosylation. Other residues, with p$K_a$ values between the two physiological pH values, will contribute to the pH-dependent functions of the nitrophorins, and others will remain neutral at these pH values because they have high p$K_a$s. In addition, because many of the carboxyl side chains may be ion paired with lysine or arginine side chains this 'salt bridge' will not contribute to the $E_m$ (though mutation of one of the residues in a salt bridge may result in the contribution from its partner's charge to the mutant's $E_m$ if this partner remains charged). To distinguish each of these different contributions we would need to know the p$K_a$ values of each of these residues. Ongoing solution NMR investigations will determine these values for NP2. For NP4 they have been estimated from high-resolution crystals structures,[36,92] which suggest that the only residues that change protonation state in NP4 are Asp27, Asp30, His124, and Asp132 for water-bound (pH 5.6) relative to NH$_3$-bound (pH 7.4). However, it should be noted that many of the ferric NO-bound structures have been photoreduced to ferrous NO complexes in the X-ray beam. Reduction of the iron center would certainly shift the p$K_a$ values of ionizable residues far more significantly than NO binding for if the residue is close enough to stabilize the net + charge on the Fe(III) then the + charge on Fe(III) is close enough to stabilize the negative charge on the residue and thus shift the p$K_a$ lower.

The p$K_a$ values (of the oxidized protein) can also be estimated from the pH dependence of the $E_m$ for these mutants since the $E_m$ will be sensitive to the charge on the residue. The pH dependence of the $E_m$ will be almost linear because it comprises a number of overlapping p$K_a$ transitions, one for each titratable residue (Figure 2d). The same will be true for each of the mutants, except that they will contain one less contribution, that of the mutated residue. Thus, the pH dependence of $\Delta E_m$ (eq 9) will depend primarily on the p$K_a$ of the mutated residue, assuming that no significant changes to other p$K_a$ values have been caused by the mutation. A plot of $E_m$ versus pH for the NO-bound mutant NP2-D1A,D89A is shown in Figure 2c, and in Figure 2e is shown the *change* in $E_m$ relative to NP2-D1A ($\Delta E_m = E_{m(NP2-D1A,D89A)} - E_{m(NP2-D1A)}$). With NO bound at pH

5.5 this mutant shows a *positive* shift of only 3 mV, indicating that D89 is likely protonated and neutral at low pH, whereas at pH 7.5 we observe a *positive* shift of 37 mV for the mutant relative to wild type. Thus, the *presence* of D89 in the wild-type protein is responsible for a *negative* contribution to the midpoint potential as would be expected for a negatively charged carboxylate side chain.

As expected, analysis of the ligand-free (water bound) $E_m$s with respect to pH is challenging because the stabilization of the Fe(III) center in the hydrophilic (relative to the NO-bound form) water-filled pocket is sensitive to other factors in addition to the charge on the mutated residue. As an example, the NP2-D1A,K127A mutant, in which we removed one lysine group relative to our reference (NP2-D1A) shows unexpected changes in $E_m$s. At *low pH* we would expect the lysine side-chain amine group to be protonated in NP2-D1A; thus, in the NP2-D1A,K127A mutant a positive charge would be removed and we would expect to see a more *negative* $E_m$, whereas the $E_m$s observed at pH 5.5 and 6.5 in the absence of NO are almost unchanged with respect to NP2-D1A. At *neutral pH* we might expect the lysine side-chain amine group to be deprotonated in NP2-D1A (or at least some increasing fraction deprotonated at higher pH, depending on its p$K_a$). Thus, we would expect to see the *least* change in $E_m$ for this mutant at neutral pH, whereas the midpoint potential observed at pH 7.5 in the absence of NO is 54 mV *more negative* (with respect to NP2-D1A). This is much larger than would be expected for a side-chain amine group that is typically over 13 Å from the Fe. Given that this change is not observed at low pH, the large negative shift in $E_m$ at pH 7.5 suggests instead that the water molecule bound to the iron of the NO-off form of NP2-D1A,K127A may deprotonate between pH 6.5 and 7.5 (with a *negative* shift of 54 mV in $E_m$ over this pH unit). The p$K_a$ of that bound water molecule for the M0-containing form of NP2 is about 10.5[24] (thus *no change* in $E_m$ between pH 6.5 and 7.5, within experimental error, is expected from deprotonation of the Fe$^{III}$−OH$_2$ for NP2-D1A). Thus, we hypothesize that the loss of the positive charge of K127 may make this mutant more susceptible to deprotonation than is M0-containing NP2 or the NP2-D1A reference of this study or any of its carboxyl mutants. In contrast to the water-bound K127A mutant, the NO complex of NP2-D1A,K127A behaves more as expected for removal of a protonatable amine group. Thus, for the NP2-D1A,K127A mutant with NO bound at pH 7.5 no change in $E_m$ is observed, as expected if its side-chain amine group were neutral at this pH (Figure 2f, plot of pH against $\Delta E_{m,NO}$). At pH 5.5, where we would expect the side-chain amine group to be positively charged in NP2-D1A, we observe a *negative* shift of 27 mV for the NP-D1A,K127A mutant relative to NP2-D1A; thus, the *presence* of K127 in the NP2-D1A protein (at low pH with NO bound) is responsible for a *positive* contribution to the midpoint potential of 27 mV due to the fact that its amine side chain is protonated at pH 5.5. As shown in Figure 2f, Table 3, and Supporting Information Figure S2.l we estimate the p$K_a$ of K127 in the NP2-D1A protein complexed to NO to be 5.4 ± 0.4.

We developed a simple approach that uses the ionizable groups' protonation/deprotonation to measure their contribution to $E_m$. Assuming that the mutated residues are mostly protonated at pH 5.5 and deprotonated at pH 7.5 (the approximate pH of the insect's salivary glands and approximate physiological pH in the tissues of the victim, respectively) the change in $\Delta E_m$ between these two pH values represents the contribution to $E_m$ that is a result of the ionization of the mutated residue only

(92) Menyhard, D. K.; Keseru, G. M. *FEBS Lett.* **2005**, *579*, 5392–5398.

$$\Delta_{pH}\Delta E_m = \Delta E_m(pH\ 7.5) - \Delta E_m(pH\ 5.5) \qquad (11)$$

A plot of $\Delta_{pH}\Delta E_m$ versus distance $r_{ij}$ is shown in Figure 4 (using $\Delta E_m$ from the NO-bound $E_{m,NO}$ values from Table 1) and summarized in Table 2. (Further discussion of the calculation of $\Delta_{pH}\Delta E_{m,NO}$ as a function of $\varepsilon_{eff}$ and the individual $E_m$ vs pH curves is provided in the Supporting Information.) As can be seen, within experimental error, almost all of the $\Delta_{pH}\Delta E_{m,NO}$ values occur between those expected for an $\varepsilon_{eff}$ of 20 and $\varepsilon_{eff}(r_{ij})$.[52−54] The equivalent buried carboxyl mutants (E53Q in NP2-D1A and E55Q in M0-containing NP1 and NP4) all have the same $\Delta_{pH}\Delta E_m$ (within experimental error), as is also true of the equivalent mutants NP2-D1A,D29A and NP4-D30A.

One of the residues that does not follow the correlation in Figure 4 is the E124A mutant of NP2-D1A (with the distance from Fe varying significantly, ranging from 7.35 to 12.95 Å, structures 2EU7 and 2ASN, respectively). It shows almost no change in $E_m$ at any pH with NO bound. The mutated E residue in NP2-D1A,E124A is thus likely protonated at all pH values investigated in this study. In contrast, all of the other residues mutated in this study undergo significant change in protonation between pH 7.5 and 5.5 and thus must have p$K_a$ values within this range. It is clear that although their p$K_a$ values may differ any charge on these residues will collectively contribute in a distance-dependent manner to the nitrophorins' $E_m$ values, and because of their close proximity, E53 and D29 (E55 and D30 in NP1 and NP4) are the most important contributors to the NP $E_m$.
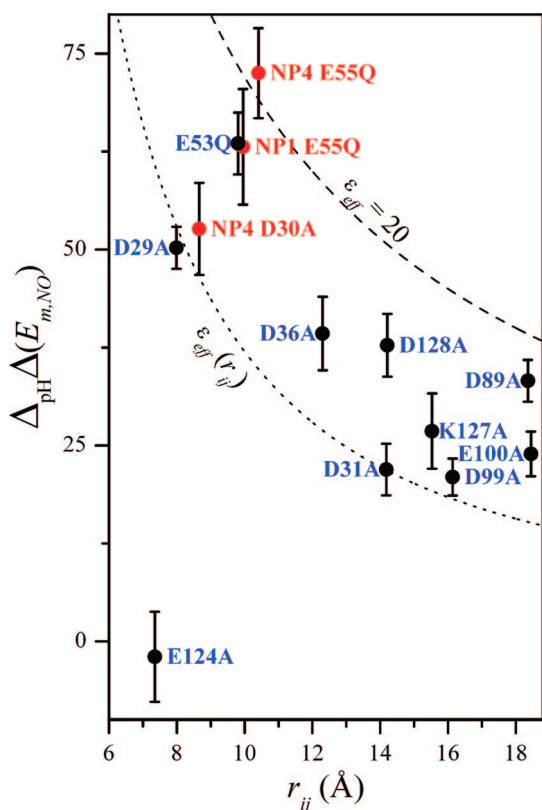
**Table 2.** Changes in Midpoint Potentials of NO Complexes (from Table 1), Charge−Charge Distances, and Approximate p$K_a$ Values for All Charge Mutants[a]

| | $\Delta_{pH}\Delta(E_{m,NO})$[b] | $r_{ij}$ (Å)[c] | p$K_a$[d] |
|---|---|---|---|
| NP2-D1A,D29A | 50 ± 3 | 7.99 | 5.4 |
| NP4-D30A | 53 ± 6 | 8.66 | 5.5 |
| NP2-D1A,D31A | 22 ± 3 | 14.18 | 7.9 |
| NP2-D1A,D36A | 39 ± 5 | 12.30 | 5.5 |
| NP1-E55Q | 63 ± 7 | 9.96[e] | 5.8 |
| NP2-D1A,E53Q | 64 ± 4 | 9.81 | 5.8 |
| NP4-E55Q | 73 ± 6 | 10.41 | 6.7 |
| NP2-D1A,D89A | 33 ± 3 | 18.36 | 7.2 |
| NP2-D1A,D99A | 21 ± 2 | 16.14 | 7.8 |
| NP2-D1A,E100A | 24 ± 3 | 18.45 | 7.5 |
| NP2-D1A,E124A | −2 ± 6 | 7.35 | f |
| NP2-D1A,K127A | 27 ± 5 | 15.53 | 5.4 |
| NP2-D1A,D128A | 38 ± 4 | 14.21 | 7.4 |

[a] Midpoint potentials in millivolts; measured at 27 °C. [b] From Table 1, $\Delta_{pH}\Delta(E_{m,NO}) = \Delta E_{m,NO}(pH\ 7.5) - \Delta E_{m,NO}(pH\ 5.5)$. [c] Distances from O/N to Fe taken from NP2-D1A crystal structure PDB file 2EU7 (NP1 file 2NP1; NP4 file 1X8P). [d] Estimated by fitting $\Delta E_{m,NO}$ vs pH (from Table 1) using eq 12 as described in the Supporting Information; error estimated to be ±0.4. [e] Average charge−charge distance for the two molecules in the unit cell. [f] Apparently protonated at all pH values investigated (with NO bound).

As discussed previously and shown in Figure 4, the response in midpoint potential just between pH 5.5 and 7.5 is fairly consistent with a simple charge−charge interaction (eq 6). However, it should be noted that this change in potential is an underestimate of the total contribution caused by the charge on the side chain because this is only the change between pH 5.5 and 7.5. Thus, because of partial ionization, $q_j$ cannot be assumed to be 0 at pH 5.5 and −1 at pH 7.5. The 'full' contribution of unit net charge could be obtained from the amplitude of the p$K_a$ fit to these data if the intrinsic p$K_a$ of the residue were known accurately, such as by NMR measurements. Clearly, the contribution to the midpoint potential by these selected residues is very significant over this pH range. Taken together, the total pH dependence of the $E_m$ should be very large, much larger than the pH dependence observed for NP2-D1A(NO) (with a 34 mV/pH unit negative shift over the pH 5.5−7.5 range). Thus, other ionizable residues (some of which may form salt bridges with the residues of this study) must neutralize many of these contributions. The nitrophorins are thus protected from autoreduction at the physiological pH of the blood and/or tissues of the host by the cumulative contributions of many negatively charged residues at various distances from the Fe center that together keep the midpoint potential low. However, at the low pH in the insect's salivary gland many of these residues are protonated, and thus other mechanism(s) must maintain the low $E_m$, including partial charges on some carboxyls that are quite close to Fe that have low p$K_a$ values. This mechanism is still dependent on some of the protonated residues, as is apparent for the NO-bound midpoint potentials. At low pH many mutants have negative shifts (typically only about −10 mV, Table 1), suggesting that these residues are involved in extensive hydrogen-bonding networks that not only affect the protonation state of other residues but likely change the position and access of water molecules to the heme pocket. The precise position of these polar water molecules with respect to the Fe center must significantly affect the midpoint potentials as they are able to approach very closely and stabilize $Fe^{III}$ relative to the $Fe^{II}$ state.

As discussed in detail in the Supporting Information, the 'full' contribution to $E_m$ that arises from net unit charge ($q_j = -1$ for



**Figure 4.** $\Delta_{pH}\Delta E_m$ ($\Delta E_{m,(pH7.5)} - \Delta E_{m,(pH5.5)}$) for the NO-bound mutants at pH 7.5 plotted against the distance of Fe to closest O/N of the mutated carboxyl/amine side chain (using the NP2-D1A crystal structure PDB file 2EU7 (NP1 structure, PDB file 2NP1, NP4: PDB file 1X8P) with NP2-D1A mutants in blue and NP1 and NP4 mutants in red (Table 2). The dashed lines represent the boundaries of the region covered for eq 6 by the distance-dependent effective dielectric constant of Schutz and Warshel, $\varepsilon_{eff}(r_{ij})$,[53] which is given by eq 10[52−54] and an effective dielectric constant $\varepsilon_{eff}$ = 20.

carboxylates) for a mutated residue is equivalent to the amplitude of the $pK_a$ fit to the pH vs $\Delta E_{m,NO}$ plot. This amplitude can be calculated using the distances from the appropriate X-ray structure and a good estimate of $\varepsilon_{eff}$ (assuming that the X-ray structure distances are the same in solution and that the mutation causes no other changes in $pK_a$ that affect $E_m$ significantly). This calculated amplitude ($\Delta E_{amp}$) for each residue then allows estimation of the $pK_a$ for each by least-squares fitting the measured $\Delta E_m$ at each pH using the equation

$$\Delta E_m(pH) = \{\Delta E_{max}(10^{pH-pK_a}) + (\Delta E_{max} - \Delta E_{amp})\}/ (1 + 10^{pH-pK_a}) \quad (12)$$

In this equation $\Delta E_{max}$ is the maximum midpoint potential and $\Delta E_{amp}$ is the amplitude of the $pK_a$ titration that is calculated using eq 6 and an $\varepsilon_{eff}$ of 15 (an optimal value of $15 \pm 3$ was found for our system, as shown in the Supporting Information). Thus, only two fitting parameters are used to fit the measured $\Delta E_{m,NO}$ for each pH value. Although the $pK_a$ value that is determined by this method is probably not exact (we estimate the accuracy as $\pm 0.4$ $pK_a$ units), it is at least as reliable as trying to detect the presence of protons from C—O bond lengths in carboxyl groups by X-ray crystallography and enables us to place each residue into a category (Table 2; $pK_a$ values determined for each of the mutated residues in the NO-bound form). Many of the $pK_a$ values summarized in Table 2 are shifted from the 'textbook' $pK_a$s once generally accepted. However, it is becoming increasingly clear that many residues, even residues on the surface of proteins, can have dramatically shifted $pK_a$ values.[93]

As can be seen from Table 2, all three of the equivalent E53/E55 carboxyls are ionized at neutral pH and at least partially ionized at low pH (5.5), though not as much for the equivalent NP4 residue E55, which has a $pK_a$ that is 0.9 units higher than that of E53 of NP2-D1A when bound to NO. Due to their close proximity to the heme all three E53/55 carboxyls contribute significantly to lowering the midpoint potentials of the three nitrophorins studied at both pH values. The same is true of D29 in NP2 and the equivalent NP4 residue D30, which are both also in very close proximity to the heme. Of the residues studied only E124 appears to be fully protonated at both pH values. All of the others are significantly ionized at pH 7.5 (and pH 5.5 for K127) and, unless neutralized by a salt bridge, contribute to the nitrophorins' low $E_m$ values.

**Crystal Structure of NP4-E55Q(NH3).** The crystal structure of the NP4 mutant E55Q was determined to help understand the role of E55(53) in nitrophorin function. The glutamate at position 55 in NP4 (53 in NP2) is conserved in the *Rhodnius* nitrophorins, but its role in nitrophorin function has been a mystery. The residue is buried in the protein interior, an unusual location for a charged residue (Figure 5a). In wild-type NP4 Glu 55 can occupy two conformations and two solvation states, one through water and one through hydrogen bonding and weak electrostatic stabilization with Phe 107 (Figure 5b and 5c). These two states vary with pH, leading to the suggestion that one is protonated and the other not.[34−36] Both wild-type and mutant have E55 (Q55) also hydrogen-bonding to Y105 (O—O = 3.19 Å for Gln 55, 2.77 Å for Glu 55). Gln 55 also has a direct H-bond from Y17-OH to the amide N of Q55 (O-N = 2.79 Å). In NP2, Glu 53 occupies a similar interior position but is stabilized through a different hydrogen-bonding arrangement[30] in which Glu 53 makes two hydrogen bonds with the −OH groups of the nonconserved Y81 (O—O = 2.66 Å) and Y104

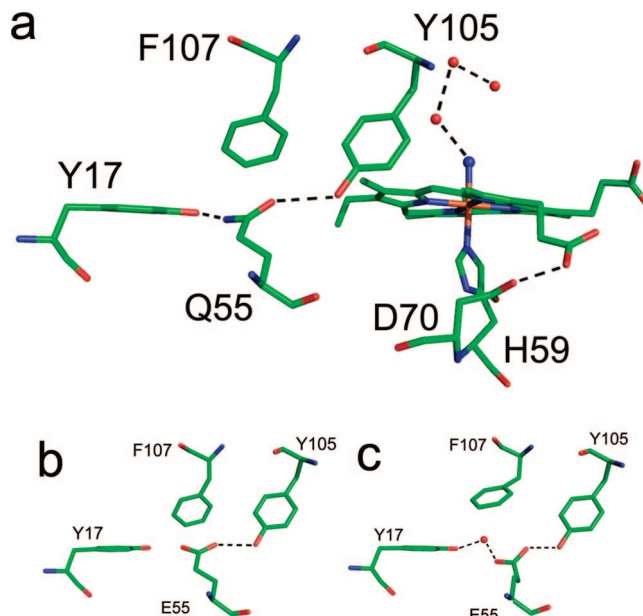(93) Harris, T. K.; Turner, G. J. *IUBMB Life* **2002**, *53*, 85−98.

**Figure 5.** (a) E55Q mutant showing hydrogen bonds to Y105 (3.2 Å) and Y17 (2.8 Å). (b and c) Wild-type protein at pH 7. Two arrangements are seen, most likely representing protonated and unprotonated E55. (b) Arrangement is nearly identical to that for Q55 except for a slight rotation of E55 (0.9 Å for the carbonyl oxygen) and Y17 (1.3 Å for the hydroxyl). (c) F107 rotates substantially (3.8 Å for ring carbon CZ) to allow a solvent molecule to enter and solvate E55, which is probably in the deprotonated state. These two arrangements are discussed elsewhere in more detail.[34−37]

(O—O = 2.35 Å (PDB file 1EUO). Y17 is not within hydrogen-bonding distance to Glu 53 (O—O = 4.35 Å), but the carboxylate forms a weak hydrogen bond to Y81 (O—O = 3.12 Å). For two D1A mutant structures and the M0-containing NP2 structure the closest distance between the E53-COO⁻ and Fe differs by 0.30 Å (9.81, 10.10, and 9.86 Å (PDB files 2EU7, 2ASN, and 1EUO, respectively).

The crystal structure of NP4 E55Q confirms that residue Gln 55 resides in a nearly identical position to one of the Glu 55 conformations in the wild-type protein, that for the arrangement without the solvating water molecule (Figure 5b), which we believe to have a protonated Glu 55. There is a slight collapse in the pocket, which allows for two excellent hydrogen bonds for Gln 55 (Figure 5a). Gln 55 and nearby residues are well ordered in the structure and occupy a single conformation. Overall, the E55Q structure is very similar to that of the wt NH3 complex, in that it displays an open heme pocket and high mobility in the A−B loop.

The buried carboxyl group, E53 (E55 in NP1 and NP4), plus D29 (D30 in NP4) are the most important charged group contributors to the $E_m$s of the nitrophorins, not only because of their close proximity to the heme, but also because they have the lowest $pK_a$s of their carboxyl groups found in this study. Thus, they are fully ionized at neutral pH and at least partially ionized at low pH in the salivary gland of the insect. To a smaller extent, this is also true of a number of other NP2-D1A carboxyl mutants, including those with charges exposed to the aqueous medium. However, because most of these are much further from the heme and they have greater fractions protonated because of higher $pK_a$s, their contributions to $E_m$ are smaller (Figure 4 as compared to Figure 3). What is immediately apparent is that when the buried charge in NP2 (E53) is removed by mutation to Q, a large change in $E_m$ occurs ($\Delta E_{m,NO}$ = +104

mV at pH 7.5, Table 1). The $pK_a$ of this residue is about 5.8, and so it is fully ionized at pH 7.5 ($q_j = -1$). Thus, based on eq 6 its charge—charge interaction with the oxidized heme (the Fe of which has $q_i = +1$) is consistent with an $\varepsilon_{eff}$ of 14 (see Supporting Information). At pH 5.5 slightly more than one-half of the E53 residues will be protonated in solution, which is consistent with a smaller change in $E_m$ for this mutation at this pH ($\Delta E_{m,NO} = +40$ mV at pH 5.5). The equivalent buried carboxyl E55 in NP1 and NP4 has a similar $pK_a$ (5.8 and 6.7, respectively, Table 2), and thus a similar contribution to $E_m$ (measured as the change in $\Delta E_m$ between pH 5.5 and 7.5, $\Delta_{pH}\Delta(E_{m,NO})$ in Table 2 and Figure 4). Although the contribution to $E_m$ due to the *charge* on the nitrophorins' buried carboxylates is the same (pH-dependent contribution), the $\Delta E_m$ values for M0-containing NP1(NO) and NP4(NO) are much more negative than for NP2-D1A(NO); in fact, the $\Delta E_m$ for NP1-E55Q(NO) at pH 5.5 is $-55$ mV (Table 1). This negative contribution, the opposite to what would be expected for removing a negative charge, is likely due to changes in the hydrogen-bonding network associated with E55, which may move a buried water molecule closer to the iron center or cause some other structural change that would stabilize the Fe(III) state of these proteins.

Thus, it appears that NP2, and likely the other nitrophorins as well, are optimally designed to stabilize the Fe(III) state of these proteins using a fairly large number of small- to intermediate-sized contributions from charged side chains rather than investing all of the stability of the oxidized state of iron in one "magic bullet" residue. The fact that most are only partially ionized at pH 7.5 explains the deviations in Figure 3, with many having a lower contribution than expected for their distance from the iron. This is an optimal design for a biological system in order to avoid the situation in which a single fatal mutation could reverse the stability of the two iron oxidation states. When the residue with the largest effect, E53(55), is mutated to Q, the protein is severely destabilized and both wild-type NP2-E53A and -E53Q cannot be folded (Berry, R. E. Unpublished work). However, NP2-D1A,E53Q can be folded, and the holoprotein is reasonably stable when bound to NO, but is not stable at lower pH (6.5, 5.5) in the absence of NO.

**Equilibrium Constants for NO Binding to the NP2-D1A Carboxyl and Amine Mutants.** Since NO is released in the tissues of the victim, which range in pH from 7.2 to 7.5,[94] we measured the equilibrium constants for NO binding to NP2-D1A and its mutants at pH 7.5. An example of the spectral changes and fit to eq 7 is shown in Figure 6 for the NP2-D1A,D128A mutant, for which the $\log_{10} K_f^{III}{}_{NO}$ is $8.1 \pm 0.1$ $\log_{10}$ M$^{-1}$. The formation constants, as $\log_{10} K_f^{III}{}_{NO}$, and calculated $\log_{10} K_f^{II}{}_{NO}$ values from eq 5 (using the $E_{m,NO} - E_m$ difference from the values in Table 1 and the measured $\log_{10} K_f^{III}{}_{NO}$ values) are presented in Table 3. Each of the nitrophorins in the ferric form has a very different NO formation constant (as observed previously at pH 8.0[17]), smallest for M0-containing NP1 ($\log K_f^{III}{}_{NO} = 6.0$ or formation constant $K_f = 1 \times 10^6$ M$^{-1}$ and dissociation constant $K_d$ of 1 $\mu$M), and largest for M0-containing NP2 ($\log K_f^{III}{}_{NO} = 8.3$, $K_f^{III} = 2 \times 10^8$ M$^{-1}$, $K_d$ of 5 nM). These differences and the corresponding differences in NO-off rates are believed to spread out the time over which NO is released in the tissues of the victim.[17] NP2-D1A has the same NO complex formation constant as M0-containing

(94) Boron, W. F.; Boulpaep, E. L. *Medical Physiology: A Cellular And Molecular Approach*; Elsevier/Saunders: Philadelphia, PA, 2005; p 634.
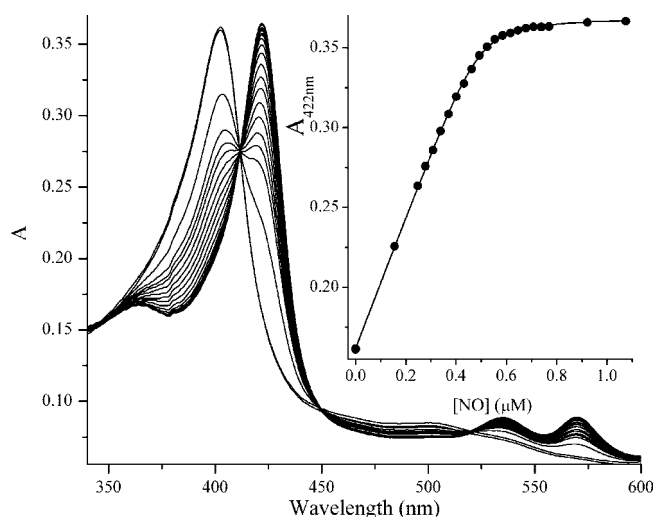


**Figure 6.** Spectrophotometric titration of NP2-D1A,D128A with NO at pH 7.5, 27 °C. The fit of the data to eq 8 is shown in the inset and yields a value of $\log_{10} K_f^{III}{}_{NO} = 8.1 \pm 0.1$ $\log_{10}$ M$^{-1}$ (Table 3).

**Table 3.** Nitric Oxide Binding Constants for Nitrophorins and Their Charge Mutants at pH 7.5[a]

| | log $K_f^{III}{}_{NO}$ | log $K_f^{II}{}_{NO}$[b] | ref |
|---|---|---|---|
| NP1 | $6.0 \pm 0.1^c$ | $13.3 \pm 0.1$ | TW |
| NP2-M0D1[e] | $8.3 \pm 0.1^c$ | $13.6 \pm 0.1$ | 20 |
| NP2-D1A | $8.3 \pm 0.1$ | $13.4 \pm 0.1$ | 20 |
| NP4 | $6.7 \pm 0.1^c$ | $12.4 \pm 0.1$ | TW |
| NP2-D1A,<u>D29A</u> | $8.0 \pm 0.2$ | $13.3 \pm 0.2$ | TW |
| NP4-<u>D30A</u> | $d$ | | TW |
| NP2-D1A,<u>D31A</u> | $8.0 \pm 0.1$ | $14.0 \pm 0.1$ | TW |
| NP2-D1A,D36A | $8.3 \pm 0.1$ | $13.6 \pm 0.1$ | TW |
| NP1-<u>E55Q</u> | $7.1 \pm 0.3$ | $13.3 \pm 0.3$ | TW |
| NP2-D1A,<u>E53Q</u> | $7.3 \pm 0.1$ | $14.1 \pm 0.1$ | TW |
| NP4-<u>E55Q</u> | $6.7 \pm 0.2$ | $12.1 \pm 0.2$ | TW |
| NP2-D1A,<u>D89A</u> | $8.3 \pm 0.1$ | $14.0 \pm 0.1$ | TW |
| NP2-D1A,D99A | $8.0 \pm 0.1$ | $13.6 \pm 0.1$ | TW |
| NP2-D1A,E100A | $8.3 \pm 0.1$ | $14.3 \pm 0.1$ | TW |
| NP2-D1A,E124A | $8.0 \pm 0.1$ | $13.1 \pm 0.1$ | TW |
| NP2-D1A,<u>K127A</u> | $8.4 \pm 0.1$ | $14.5 \pm 0.1$ | TW |
| NP2-D1A,<u>D128A</u> | $8.1 \pm 0.1$ | $14.6 \pm 0.1$ | TW |

$^a$ Binding constants in $\log_{10}$ M$^{-1}$, measured at 27 °C; conserved amino acids underlined. $^b$ Calculate $\log_{10} K_f^{II}{}_{NO}$ values from eq 5 (used the $E_{m,NO} - E_m$ difference from the values in Table 1). $^c$ These values were previously determined at pH 8.0 (ref 17) with values of 6.1, 7.7, and 6.3, for NP1, NP2-M0D1, and NP4, respectively. TW: This work. $^d$ Could not be determined due to iron reduction during the NO titration. $^e$ The M0D1 label refers to expression with the N-terminal methionine present, while the D1A mutant does not have M0 present.[20]

NP2, and most of the NP2-D1A-containing mutants have similarly large NO formation constants, indicating that the negative charges of these carboxylates stabilize the Fe$^{III}$(H$_2$O) and Fe$^{III}$(NO) states equally.

The exception is the $K_f$ of the mutant NP2-D1A,E53Q, which is a full power of 10 smaller than that of the wild-type or NP2-D1A mutant. Thus, removal of the negative charge of the buried carboxylate, E53, in NP2 *destabilizes* the Fe$^{III}$(NO) complex. The opposite situation exists for the equivalent NP1 mutant E55Q, where $K_f$ is a full power of 10 larger than that of the wild type; thus, in M0-containing NP1 removal of the negative charge of E55 stabilizes the Fe$^{III}$(NO) complex relative to the Fe$^{III}$(H$_2$O) state. For NP4-E55Q no change in NO formation constant is observed relative to NP4 wild type. In fact, all three equivalent buried carboxylate mutants have similar NO binding constants (the corresponding $K_d$s range from 200 to 50 nM, a

factor of 4 difference) as compared to wild type ($K_d$s range from 1000 to 5 nM, a factor of 200 difference). Thus, by some mechanism E53/E55 is involved with regulation of the nitrophorins' NO binding affinities to the ferric forms of the proteins, possibly through the differing roles of water molecules in the distal pocket and the possibility that the water bound to Fe has a different $pK_a$ in the three NPs of this study. Although the $pK_a$ of the water bound to M0-containing NP2 has been measured $(10.5 \pm 0.2)$,[24] and is too high to affect NO binding at pH 7.5 or lower, those of NP2-D1A, NP1, and NP4 as well as their E53(55)Q mutants have not been measured.

For the ferrous NO complexes, while the M0-containing wild-type and D1A mutant of NP2 and the M0-containing NP1 have formation constants for the $Fe^{II}(NO)$ complexes almost within experimental error of each other, only some of the mutants have this size ($\log_{10} K_f^{II}{}_{NO} = 13.3-13.6 \pm 0.1 \log_{10} M^{-1}$), i.e., the D29A, D36A, D99A, and E124A mutants of NP2-D1A and NP1-E55Q. NP4 and its mutant E55Q also have formation constants within experimental error of each other, though with values of $\log_{10} K_f^{II}{}_{NO}$ 10 times smaller than those of NP1 and NP2. Most of the others, including the D31A, E53Q, D89A, E100A, K127A, and D128A mutants of NP2-D1A, have significantly increased values of $\log_{10} K_f^{II}{}_{NO}$ that range from 14.0 to 14.6 $\log_{10} M^{-1}$. K127 and D128 have the mutation far from the metal but not the farthest. Thus, removal of a negative charge *stabilizes* the $Fe^{II}(NO)$ complex (relative to the $Fe^{II}$ NO-off state, which is not expected to have a water bound), where there is no formal positive charge on the iron, and the same stabilization exists for the K127A mutant, where a positive charge is removed.

It is also interesting to note that most of these mutants also have large negative shifts in $E_m$ (D31A, E100A, K127A, and D128A have $\Delta E_m$ of ca. $-40$ mV at pH 7.5). Thus, removal of the charge also *stabilizes* the $Fe^{III}(H_2O)$ state (or $Fe^{III}(OH)$ in some cases[95]) relative to the $Fe^{II}$ state. From cursory study of the protein structure it is not clear why removing these negative and positive charges destabilizes the five-coordinate high-spin Fe(II) state relative to both the $Fe^{II}(NO)$ and $Fe^{III}(H_2O/OH)$[95] states, and theoretical calculations will be needed to understand these results. The binding constant for NO to NP4-D30A could not be measured because of autoreduction of this mutant during the NO titration, which is not surprising considering that this mutant has the highest $E_{m,NO}$ value of any of the nitrophorin mutants studied so far (+198 mV). In terms of the structure and kinetics properties, this mutant also does not close the A−B loop properly and has lost the pH dependence for NO binding (through the off-rate).[35] Thus, one of the most important functions of this residue is maintaining the NP(NO) complex in the ferric form. It should be noted that binding constants of NO to the Fe(II) form of these proteins of $10^{13.3}$, $10^{13.4}$, and $10^{12.4}$ $M^{-1}$ represent 50, 40, and 400 fM $K_d$s for the NO complexes of NP1, NP2-D1A, and NP4, respectively, as compared to those for the Fe(III) form of these proteins (where the NO binding constants range from $10^6$, $10^{8.3}$, and $10^{6.7}$ $M^{-1}$, which represent 1000, 5, and 200 nM $K_d$s, respectively). These are factors of about a million larger than those of the Fe(II) forms, which indicate that maintaining the NP-NO complex in the Fe(III) oxidation state is vital to the insect's success in using nitric oxide to obtain a sufficient blood meal.

(95) As mentioned above, the $pK_a$ of the water molecule bound to Fe(III) in M0-containing NP2 is $10.5 \pm 0.2$.[24] However, for the NP2-D1A,K127A mutant the $pK_a$ of that water molecule appears to be lowered considerably to near 8.0 (unpublished results).
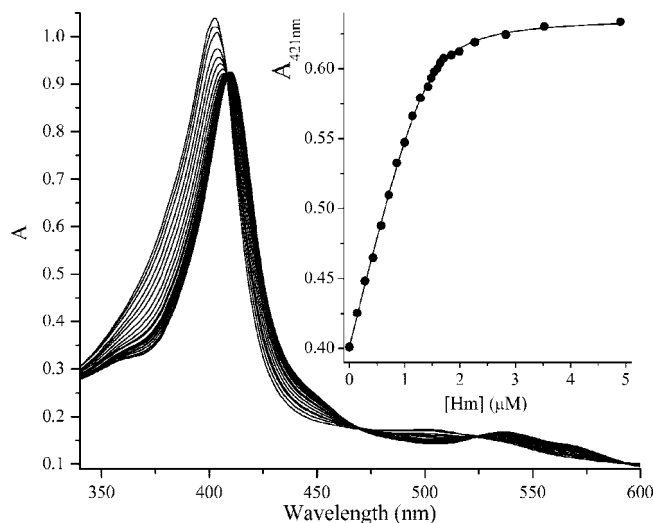


**Figure 7.** Spectrophotometric titration of NP2-D1A,D128A with histamine at pH 7.5, 27 °C. The fit of the data to eq 8 is shown in the inset and yields a value of $\log_{10} K_f^{III}{}_{Hm} = 7.1 \pm 0.1 \log_{10} M^{-1}$ (Table 4).

**Equilibrium Constants for Histamine and Imidazole Binding to the NP2-D1A Carboxyl Mutants.** The other physiologically important ligand for the nitrophorins is histamine, which is released by platelets and mast cells of the victim in response to the bite. Thus, we measured the binding constants of histamine (Hm) and its simpler model imidazole (ImH) to the nitrophorins. An example of the titration data for histamine binding to the Fe(III) state of NP2-D1A,D128A and the fit to the data to yield the log $K_f^{III}$ is shown in Figure 7. All binding constants for both of these ligands at pH 5.5 and 7.5 are collected in Table 4. The histamine binding constants to M0-containing NP2, NP2-D1A, and M0-containing NP1 and NP4 are identical within experimental error (Table 4) and at pH 7.5 are within a factor of 2 (for NP2-D1A) to orders of magnitude greater (for NP1 and NP4) than those for NO binding (Table 3). Thus, in the tissues of the victim the two ligands, if at equal concentrations, can compete for the Fe(III) binding site. Histamine binding constants are in general larger than those of imidazole by about 1 log unit.

The imidazole binding constants for all of the mutants, compared to their wild-type values, are generally slightly smaller at pH 7.5 and larger at pH 5.5 (most notably for NP1-E55Q and NP4-E55Q with 1 log unit increases at pH 5.5), the exceptions being NP2-D1A,E124A with an increase in imidazole binding constant at both pH values by 0.7 log units. Histamine binding constants are generally smaller for all of the carboxyl mutants at both pH values (especially at pH 7.5), most notably for NP2-D1A,D29A at pH 7.5, where the binding constant of imidazole is 1.3 log units larger than that of histamine. Deprotonated D29 probably acts as H-bond acceptor from the protonated amine group of histamine, for as seen in the crystal structure of NP1-histamine it is optimally positioned to do so; a preliminary unpublished structure of NP2-D1A(Hm) confirms this. The equivalent D30 carboxyl of NP1 forms a good hydrogen bond to the protonated amino nitrogen of histamine (2.73 Å) as do the backbone carbonyls of E32 and L130 (2.83 and 2.70 Å, respectively) (PDB file 1NP1). Thus, the loss of that hydrogen-bonding interaction would severely weaken the binding of histamine, which is then simply a significantly larger ligand than imidazole and thus has a smaller binding constant, especially at pH 7.5. The equivalent mutant NP4-D30A shows a small change in imidazole binding constant compared to NP4

***Table 4.*** Binding Constants for Histamine and Imidazole to the Nitrophorins and Their Charge Mutants[a]

| | pH | log $K_f^{III}{}_{Hm}$ | log $K_f^{III}{}_{ImH}$ | ref |
|---|---|---|---|---|
| NP1 | 5.5 | $6.6 \pm 0.1$ | $5.7 \pm 0.1$ | 19 |
| | 7.5 | $8.0 \pm 0.1$ | $6.9 \pm 0.1$ | 19 |
| NP2-M0D1 | 5.5 | $6.6 \pm 0.1$ | $5.5 \pm 0.1$ | 19 |
| | 7.5 | $8.0 \pm 0.1$ | $7.4 \pm 0.1$ | 19 |
| NP2-D1A | 5.5 | $6.6 \pm 0.1$ | $5.7 \pm 0.1$ | 20 |
| | 7.5 | $8.0 \pm 0.2$ | $7.4 \pm 0.1$ | 20 |
| NP4 | 5.5 | $6.6 \pm 0.1$ | $5.8 \pm 0.1$ | 19 |
| | 7.5 | $8.2 \pm 0.1$ | $6.9 \pm 0.1$ | 19 |
| NP2-D1A,<u>D29</u>A | 5.5 | $5.8 \pm 0.2$ | $5.7 \pm 0.1$ | TW |
| | 7.5 | $5.5 \pm 0.1$ | $6.8 \pm 0.4$ | TW |
| NP4-<u>D30</u>A | 5.5 | $6.0 \pm 0.1$ | $6.0 \pm 0.1$ | TW |
| | 7.5 | $6.8 \pm 0.1$ | $7.0 \pm 0.1$ | TW |
| NP2-D1A,<u>D31</u>A | 5.5 | $6.4 \pm 0.1$ | $6.1 \pm 0.1$ | TW |
| | 7.5 | $7.6 \pm 0.1$ | $7.2 \pm 0.1$ | TW |
| NP2-D1A,D36A | 5.5 | $5.6 \pm 0.1$ | $5.9 \pm 0.1$ | TW |
| | 7.5 | $7.5 \pm 0.1$ | $7.5 \pm 0.3$ | TW |
| NP1-<u>E55</u>Q | 5.5 | $6.9 \pm 0.1$ | $6.7 \pm 0.1$ | TW |
| | 7.5 | $7.8 \pm 0.1$ | $7.2 \pm 0.1$ | TW |
| NP2-D1A,<u>E53</u>Q | 5.5 | $6.9 \pm 0.1$ | $6.0 \pm 0.1$ | TW |
| | 7.5 | $7.7 \pm 0.2$ | $7.9 \pm 0.3$ | TW |
| NP4-<u>E55</u>Q | 5.5 | $7.4 \pm 0.1$ | $6.9 \pm 0.2$ | TW |
| | 7.5 | $7.5 \pm 0.1$ | $6.8 \pm 0.1$ | TW |
| NP2-D1A,<u>D89</u>A | 5.5 | $6.7 \pm 0.1$ | $5.9 \pm 0.1$ | TW |
| | 7.5 | $7.9 \pm 0.1$ | $7.3 \pm 0.1$ | TW |
| NP2-D1A,D99A | 5.5 | $6.6 \pm 0.1$ | $6.1 \pm 0.1$ | TW |
| | 7.5 | $7.7 \pm 0.2$ | $7.0 \pm 0.1$ | TW |
| NP2-D1A,E100A | 5.5 | $6.6 \pm 0.1$ | $6.0 \pm 0.1$ | TW |
| | 7.5 | $8.7 \pm 0.2$ | $7.1 \pm 0.2$ | TW |
| NP2-D1A,E124A | 5.5 | $7.1 \pm 0.1$ | $6.4 \pm 0.1$ | TW |
| | 7.5 | $7.5 \pm 0.1$ | $8.1 \pm 0.2$ | TW |
| NP2-D1A,<u>K127</u>A | 5.5 | $6.5 \pm 0.1$ | $5.8 \pm 0.1$ | TW |
| | 7.5 | $8.2 \pm 0.1$ | $7.2 \pm 0.2$ | TW |
| NP2-D1A,<u>D128</u>A | 5.5 | $6.3 \pm 0.1$ | $6.5 \pm 0.1$ | TW |
| | 7.5 | $7.1 \pm 0.1$ | $7.3 \pm 0.1$ | TW |

[a] Binding constants in $\log_{10}$ M$^{-1}$, measured at 27 °C; conserved amino acids underlined. TW: This work.

wild type, but like NP2-D1A,D29A shows a very large decrease in the histamine binding constant, especially at pH 7.5. The exception to this trend of weaker histamine binding constants for carboxyl mutants is NP2-D1A,E124A and the equivalent buried carboxyl mutants NP1-E55Q, NP2-D1A,E53Q, and NP4-E55Q, which all have larger histamine binding constants at pH 5.5, and NP2-D1A,E100A, which has a larger histamine binding constant at pH 7.5 by 0.7 log units. E100 is a hydrogen-bond acceptor from the protonated amine group of K84 (2.54 Å, PDB file 2EU7), and thus, removal of that carboxylate would allow the protonated K84 side chain to remain free or interact with either E97 or D99, all of which are on the surface of the protein; the E97A mutant has not been prepared in this work, but the D99A mutant shows no significant differences in binding constants from wild-type NP2 or its D1A mutant.

At pH 7.5, with the exceptions noted above, where most of the carboxyls are deprotonated, histamine complexes of the carboxyl mutants are *destabilized* by removal of a negative charge. This destabilization is much more significant than any for the imidazole complex of the same mutant, highlighting the unique importance of the $-NH_3^+$ side chain of histamine in its binding to the nitrophorins (most notably for NP2-D1A,D29A). At pH 5.5, where the buried carboxyl E53 (E55 in NP1 and NP4) is partially protonated, removal of this charge causes *stabilization* of both histamine and imidazole complexes. Thus, at low pH in the salivary gland where the nitrophorin must bind NO, the buried carboxyl E53 helps reduce the affinity of histamine, and at high pH in the tissues of the victim the residue

D29 (along with most of the carboxyl residues) helps increase the affinity for histamine.

## Summary and Conclusions

NP2 and the other nitrophorins are optimally designed to stabilize the Fe(III) state of the proteins via a large number of fairly small contributions from charged side chains rather than investing all of the stability of the oxidation state of iron in one residue. This provides a means of avoiding the situation in which a fatal mutation could reverse the stability of the two iron oxidation states. Thus, although E53 and D29 are responsible for a significant proportion ($\sim$50%) of the lowering of the midpoint potential of NP2-D1A, the other residues collectively contribute significantly. Another important contributor to the stability of the ferric state of the nitrophorins is ruffling of the heme caused by the distal leucines L122 and L132, which has been shown elsewhere[18] to account for a 38 mV stabilization of the oxidized state, measured as $\Delta E_m$ of the NO complexes of the L132V single and L122V,L132V double mutants, in the absence of other mutations. I120 is also of major importance to the ruffling of NP2 and NP3 as well as to their **A:B** heme ratio at equilibrium.[25]

The effect of the distance of the closest carboxylate oxygen from the iron on the midpoint potential varies roughly with distance in a manner expected from eq 6 but with an effective dielectric constant $\varepsilon_{eff}$ of approximately $15-20$ for the medium between the iron and the charged group (depending on whether the p$K_a$ of the charged group is taken into account). This range of $\varepsilon_{eff}$ is typical of what has been found by Warshel and co-workers in many detailed theoretical studies,[45,52] as well as experimental data[43,47,50,54,55] for proteins containing buried charges. It reflects a general property of proteins, i.e., that their folding energy is not large and that upon charge separation they always reorganize and provide compensation by "solvation" due to reorientation of protein polar groups and/or water penetration.[45,55] Although the heme iron is buried in the protein, there is generally one or more water molecules near it, which in homogeneous solution can probably exchange with bulk water and thus increase the polarity of the redox-active iron environment.

Histamine binding constants for the Fe(III) forms of the carboxyl mutants at pH 7.5, $K_f^{III}{}_{Hm}$, are, except for the -E100A mutant of NP2-D1A, smaller when a carboxylate charge is removed, while imidazole binding constants are reduced much less or even become *larger* when a carboxylate charge is removed, thus pointing out the importance of the protonated amino group of histamine to the binding of this biological effector. At pH 7.5, M0-containing NP2 and NP2-D1A have binding constants for NO that are only a factor of 2 larger than those for histamine, while for NP1 and NP4 the binding constants for NO are significantly smaller than those for histamine. Thus, in the tissues of the victim histamine can compete with NO for the Fe(III) binding site if the two are at equal concentrations; a flood of histamine, secreted by platelets and mast cells of the victim, would ensure dissociation of the remaining NO and binding of histamine to the nitrophorins.

**Supporting Information Available:** Section S1, Detailed discussion of the methods used to estimate the p$K_a$ values of the mutated residues; Table S1, calculated $\Delta E_{amp}$ values for each value of $\varepsilon_{eff}$, obtained using eq 6; Table S2, reduced $\chi^2$ values for each $\varepsilon_{eff}$ from the nonlinear least-squares fit to eq 12 using the calculated $\Delta E_{amp}$ values; Table S3, p$K_a$ values for each $\varepsilon_{eff}$ from the nonlinear-least-squares fit to eq 12 using the calculated $\Delta E_{amp}$ values; Table S4, distances (in Å) used in Figure 3, from closest O/N to Fe, taken from X-ray crystal structures with water or ammonia coordinated to Fe; Figure S1, plot of the reduced $\chi^2$ values against $\varepsilon_{eff}$ (at values 7 to 20); Figure S2a−l, plots showing best p$K_a$ fits for each mutant (eq 12) using amplitudes $\Delta E_{amp}$ based on $\varepsilon_{eff} = 15$. Section S2, Characterization data for the mutant proteins of this study; Table S5, Soret band maxima of the NO complexes of the ferric and ferrous proteins; Table S6, crystallographic data for NP4-E55Q(NH$_3$); NMR Spectra S1−S5 of the imidazole complexes of the proteins of this study at pH 7.0, most at 25 °C. This material is available free of charge via the Internet at http://pubs.acs.org.